

# Joint latent class trees: A Tree-Based Approach to Joint Modeling of Time-to-event and Longitudinal Data

Ningshan Zhang and Jeffrey S. Simonoff

IOMS Department, Leonard N. Stern School of Business, New York University

## Abstract

Joint modeling of longitudinal and time-to-event data provides insights into the association between the two quantities. The joint latent class modeling approach assumes that conditioning on latent class membership, the trajectories of longitudinal data such as biomarkers are independent of survival risks. Furthermore, the resulting latent classes provide a data-dependent clustering of the population, which is also of interest in clinical studies. Existing joint latent modeling approaches are parametric and suffer from high computational cost. The most common parametric approach, the joint latent class model (JLCM), further restricts analysis to using time-invariant covariates in modeling survival risks and latent class memberships. We propose a nonparametric joint latent class modeling approach based on trees (JLCT). JLCT is fast to fit, and can use time-varying covariates in all of its modeling components. We compare JLCT with JLCM on simulated data, where we show that JLCT and JLCM have similar performance when using only time-invariant covariates. Further, we demonstrate the prognostic value of using time-varying covariates in each of the modeling components, and thus display the advantage of JLCT when making predictions. We further apply JLCT to a real application, the PAQUID dataset, and demonstrate again that JLCT admits competitive prediction performance, while being orders of magnitude faster than the parametric approach JLCM.

*Keywords:* Biomarker; Conditional independence; Recursive partitioning; Survival data; Time-varying covariates.

## 1 Introduction

Clinical studies often collect three types of data on each patient: the time to the event of interest (possibly censored), the longitudinal measurements on a continuous response (for example, some sort of biomarker viewed as clinically important), and an additional set of covariates (possibly time-varying) about the patient. The clinical studies then focus on analyzing the relationship between the time-to-event and the longitudinal responses, using the additional covariates. A common approach is to jointly model the time-to-event by a survival model, while modeling the longitudinal responses using a linear mixed-effects model, with both the survival and the linear mixed-effects models potentially making use of the additional covariates.

The first and most common approach for the joint modeling problem is the shared random effects model (SREM) [Wulfsohn and Tsiatis, 1997, Henderson et al., 2000, Tsiatis and Davidian, 2004, Rizopoulos, 2010]. The name “shared random effects” comes from the modeling assumption that a set of random effects accounts for the association between longitudinal outcomes and time-to-event. In particular, the longitudinal outcomes are modeled by linear mixed-effects models [Laird and Ware, 1982], with random effects for each patient. Meanwhile, these random effects affect the hazards of the event through some parametric survival model, for example a proportional hazards model. SREM is limited in the use of covariates in the survival model, as it only allows time-invariant baseline covariates, such as a treatment indicator. To fit a SREM, the parameters of the survival model and the linear mixed-effects model are estimated together via maximum likelihood. SREM proposes a straightforward way of jointly modeling the two quantities, but it comes with high computational cost.

A different line of research focuses on the joint latent class model (JLCM) [Lin et al., 2002, Proust-Lima and Taylor, 2009, Proust-Lima et al., 2009, 2017]. JLCM assumes that the population of patients

consists of multiple latent classes. A patient’s time-to-event and longitudinal responses are independent conditioning on his or her latent class membership. In addition, JLCM assumes the latent classes are homogeneous and thus patients within a latent class follow the same survival and linear mixed-effects model. Finally, the latent class membership is modeled by a multinomial logistic regression model.

What makes JLCM interesting and different from SREM is the idea of latent class membership, which (among other things) can be used to describe disease progression in clinical studies [Lin et al., 2002, Garre et al., 2008, Proust-Lima et al., 2009]. It is well-known that many diseases have different stages; examples include dementia, AIDS, cancer, and chronic obstructive pulmonary disease (COPD) [Dicker et al., 2006]. From a clinical point of view, it is important to identify those stages, since treatment could change with membership in different stages [Hajiro et al., 2000]. Currently the clinical definitions of stages of a disease consist of using diagnostic findings (such as biomarkers) to produce clusters of patients. However, it is possible that by jointly studying biomarker trajectories and survival experiences, one can find data-dependent latent classes that uncover new, meaningful stages.

JLCM, like most frequentist parametric approaches, estimates the parameters for all modeling components via maximizing the log-likelihood function, which is a very complex process. Although the computational cost for JLCM is less than that of SREM, it is still prohibitively slow for large scale data. In addition, JLCM cannot use time-varying covariates in its latent class membership and survival models, which could greatly reduce its prediction performance.

A nonparametric approach that addresses some of these problems would be desirable, and tree-based approaches [Breiman et al., 1984] are natural candidates. It is very efficient to fit a tree, and the terminal nodes of a tree naturally represent a partition of the population. A tree-based approach for joint latent class modeling also addresses the time-invariant limitation of JLCM, since time-varying covariates can be used as the splitting variables to construct the tree. Furthermore, once a tree is constructed, it is up to the user to decide which type of survival models and which covariates to use within each terminal node, providing additional flexibility to the analyst.

In this work, we propose the joint latent class tree (JLCT) method. JLCT, like JLCM, is based on the key assumption that conditioning on latent class membership, time-to-event and longitudinal responses are independent. JLCT therefore looks for a tree-based partitioning such that within each estimated latent class defined by a terminal node, the time-to-event and longitudinal responses display a lack of association. Once the tree is constructed, we assign each observation to a latent class (i.e. terminal node), and independently fit survival and linear mixed-effects models, using the class membership information.

The rest of the paper is organized as follows. In Section 2 we introduce the setup of the joint modeling problem, and present our joint latent class tree (JLCT) method. In Sections 3 and 4 we use simulations to compare JLCT with JLCM in terms of prediction performance and running time. Finally, in Section 5 we apply JLCT to a real dataset, and demonstrate that JLCT admits competitive (or superior) prediction performance, while being orders of magnitude faster than the JLCM approach.

## 2 Constructing a tree to uncover conditional independence

### 2.1 Joint modeling setup

Assume there are  $N$  subjects in the sample. For each subject  $i$ , we observe  $n_i$  repeated measurements of a longitudinal outcome at times  $\mathbf{t}_i = (t_{i1}, \dots, t_{in_i})'$ . We denote the vector of longitudinal outcomes by  $\mathbf{Y}_i = (y_{it_{i1}}, \dots, y_{it_{in_i}})'$ . In addition, for each subject  $i$  we observe a vector of  $p$  covariates at each measurement time  $t \in \mathbf{t}_i$ ,  $\mathbf{X}_{it} = (x_{it1}, \dots, x_{itp})$ . These covariates can be either time-invariant or time-varying. Each subject is also associated with a time-to-event tuple  $(T_i, \delta_i)$ , where  $T_i$  is the time of the event, and  $\delta_i$  is the censor indicator with  $\delta_i = 0$  if subject  $i$  is censored at  $T_i$ , and  $\delta_i = 1$  otherwise.

We assume there exist  $G$  latent classes, and let  $g_{it} \in \{1, \dots, G\}$  denote the latent class membership of subject  $i$  at time  $t$ . We assume the latent class membership  $g_{it}$  is determined by a subset of covariates, denoted by  $\mathbf{X}_{it}^g$ .

The joint latent class modeling problem makes the key assumption that a patient’s time-to-event  $(T_i, \delta_i)$  and longitudinal outcomes  $(\mathbf{Y}_i)$  are independent conditioning on his or her latent class membership  $(g_{it})$ . Without controlling the latent class membership  $g_{it}$ , time-to-event and longitudinal outcomes may appear to be correlated because each is related to the latent class, but given  $g_{it}$  the two are independent of each other, and therefore the longitudinal outcomes have no prognostic value for time-to-event given the latent class. The modeling of  $(T_i, \delta_i)$  and  $\mathbf{Y}_i$  are therefore separated conditioning on  $g_{it}$ .

We assume the longitudinal outcomes come from a linear mixed-effects model:

$$y_{it} | g_{it}=g = \mathbf{X}_{it}^f \boldsymbol{\beta} + \mathbf{X}_{it}^r \mathbf{u}_g + v_i + \varepsilon_{it}, \quad \mathbf{u}_g \sim \mathcal{N}(0, \boldsymbol{\Sigma}_r), \quad v_i \sim \mathcal{N}(0, \sigma_1^2), \quad \varepsilon_{it} \sim \mathcal{N}(0, \sigma_2^2). \quad (1)$$

Here we assume the longitudinal outcomes depend on two subsets of  $\mathbf{X}_{it}$ , with  $\mathbf{X}_{it}^f$  the subset of covariates associated with a fixed effect vector  $\boldsymbol{\beta}$ , and  $\mathbf{X}_{it}^r$  the subset of covariates associated with a latent class-specific random effect vector  $\mathbf{u}_g$ . We assume the random effect vector  $\mathbf{u}_g$  is independent across latent classes  $g = 1, \dots, G$ . In addition, there is a subject-specific random intercept  $v_i$  that is independent across subjects and independent of the random effects  $\mathbf{u}_g$ . Finally, the errors  $\varepsilon_{it}$  are assumed to be independent and normally distributed with mean 0 and variance  $\sigma_2^2$ , and independent of all the random effects as well.

Conditioning on latent class membership, we assume the time-to-event tuple  $(T_i, \delta_i)$  depends on a subset of covariates  $\mathbf{X}_{it}^s$  observed at time  $t_i$ , through the extended Cox model for time-varying covariates [Cox, 1972]:

$$h_i(t|g_{it} = g) = h_{0g}(t)e^{\mathbf{X}_{it}^s \boldsymbol{\eta}_g}, \quad (2)$$

where  $\boldsymbol{\eta}_g$  is the vector of class-specific slope coefficients. Equation (2) shows a general form of the survival model given latent classes  $g_{it}$ . In practice one can restrict either  $h_{0g}(t)$  or  $\boldsymbol{\eta}_g$ , or both, to be identical across latent classes.

Tree construction requires fitting the extended Cox model using the longitudinal outcome variable as a predictor, and perhaps other time-varying covariates. In order to implement that, we convert the original data into left-truncated right-censored (LTRC) data [Andersen and Gill, 1982, Fu and Simonoff, 2017]. For each subject  $i$  and measurement time  $t$ , there is a “pseudo-observation” with  $y_{it}$ ,  $\mathbf{X}_{it}$ , and a time-to-event triplet  $(L_{it}, R_{it}, \delta_{it})$ , where  $L_{it}$  is the left-truncated time,  $R_{it}$  is the right-censored time, and  $\delta_{it}$  is the censor indicator.

We have introduced four subsets of covariates so far:  $\mathbf{X}_{it}^s$  for the latent classes,  $\mathbf{X}_{it}^f$  for the fixed effects,  $\mathbf{X}_{it}^r$  for the random effects, and  $\mathbf{X}_{it}^t$  for the time-to-event. Each of the four subsets can contain time-varying covariates, and the four subsets can be either identical, or share common covariates, or share no covariates at all.

## 2.2 Joint Latent Class Tree (JLCT) methodology

In Appendix A, we give a brief introduction to JLCM, and discuss at length its strengths and weaknesses. In this section we formally introduce JLCT, the joint latent class tree approach. Like JLCM, JLCT also assumes conditional independence of the longitudinal outcomes and the time-to-event within each latent class. Under this assumption, JLCT looks for a tree-based partitioning such that within each estimated class defined by a terminal node the time-to-event and longitudinal outcomes display a lack of association.

Tree-based methods are powerful modeling tools in statistics and data mining [Breiman et al., 1984, Hastie et al., 2001], especially because they are fast to construct, able to uncover nonlinear relationships between covariates, and intuitive and easy to explain. We consider binary trees, where each node is recursively split into two children nodes based on a splitting criterion. Often the splitting criterion ensures that the two children nodes are more “homogeneous” than their parent node. The measure of “homogeneity” varies by the method, for instance in a classification tree, the measure could be misclassification error, Gini index, or cross-entropy, while in a regression tree it could be residual sum of squares. The tree stops splitting when the node is “pure,” or when some stopping criteria are met.

The measure of “homogeneity” in JLCT is quite different from those commonly used in regression and classification trees. Our measure is based on the conditional independence between the time-to-event and the longitudinal outcomes: the more apparently independent the two variables are conditioning on the node, the more “homogeneous” the node is. To be more concrete, the splitting criterion repeatedly uses the test statistic for the hypothesis test

$$H_0 : b_y = 0, \quad \text{vs.} \quad H_1 : b_y \neq 0, \quad (3)$$

under the extended Cox model

$$h(t, \mathbf{X}_i^s, \mathbf{Y}_i) = h_0(t)e^{y_{it}b_y + \mathbf{X}_{it}^s \mathbf{b}_x}.$$

In the model above, the coefficient  $b_y$  is associated with the longitudinal outcomes  $\mathbf{Y}_i$ , and the vector of coefficients  $\mathbf{b}_x$  is associated with the set of covariates  $\mathbf{X}^s$ . Thus,  $b_y = 0$  corresponds to the longitudinal outcome having no relationship with the time-to-event in the node given the other covariates  $\mathbf{X}^s$ .

We have two obvious choices for the hypothesis test (3): the log-likelihood ratio test (LRT) or the Wald test. In this work we use the log-likelihood ratio test in all experiments; simulations indicate that the Wald test gives similar results. We will denote the test statistic of the hypothesis test as **TS**. The smaller the value of **TS** is, the less related longitudinal outcomes  $\mathbf{Y}_i$  are to the time-to-event data  $(L_{it}, R_{it}, \delta_{it})$  given the covariates  $\mathbf{X}_{it}^s$  and current node. JLCT seeks to partition observations using

covariates in  $\mathbf{X}^g$ , such that  $\mathbf{TS}$  is small within each leaf node, but stops partitioning when  $\mathbf{TS}$  is less than a specified stopping parameter  $s$ . More formally, the tree splitting procedure works as follows:

1. At the current node, compute the test statistic  $\mathbf{TS}_{\text{parent}}$ .
2. If  $\mathbf{TS}_{\text{parent}} < s$ , stop splitting. Otherwise proceed.
3. For every split variable  $X_j \in \mathbf{X}^g$ , and possible split point  $C$ ,
  - 3.1. Define two children nodes

$$R_{\text{left}}(j, C) = \{(i, t) : x_{itj} \leq C\}, \quad R_{\text{right}}(j, C) = \{(i, t) : x_{itj} > C\}.$$

- 3.2. Ignore this split if either node violates the restrictions specified in the control parameters. (Details are given near the end of this section.) Otherwise proceed.
  - 3.3. At each child node, determine the test statistics  $\mathbf{TS}_{\text{left}}(j, C)$ ,  $\mathbf{TS}_{\text{right}}(j, C)$  respectively.
  - 3.4. Compute the score  $S(j, C) = \mathbf{TS}_{\text{parent}} - \mathbf{TS}_{\text{left}}(j, C) - \mathbf{TS}_{\text{right}}(j, C)$ .
4. Scan through all pairs of  $(j, C)$  to find  $(j^*, C^*) = \arg \max_{j, C} S(j, C)$ , and split the current node on variable  $j^*$  at split point  $C^*$ .

JLCT recursively splits nodes according to the above procedure, until none of the terminal nodes can be further split.

The stopping criterion,  $\mathbf{TS}_{\text{parent}} < s$ , is based on the following property of the test statistic: under the null model  $H_0$  in (3), the distribution of  $\mathbf{TS}$  is approximately a  $\chi_1^2$  distribution. Therefore, we do not reject the null hypothesis  $H_0$  when  $\mathbf{TS}$  is smaller than a threshold associated to a desired significance level. We set  $s = 3.84$  by default, which is the 5% tail of the  $\chi_1^2$  distribution.

Standard control parameters, such as the minimal number of observations in any terminal node, the minimal improvement in the “purity” by a split, etc., also apply to the JLCT method. In addition, we introduce two control parameters that are specific to JLCT:

- Minimum number of events in any terminal node. This parameter ensures that the survival model in each terminal node is fit with meaningful survival data with enough occurrences of events (that is, uncensored observations). By default, this parameter is set to the number of covariates used for the Cox PH model.
- Upper bound on the variance of the estimated coefficients in all survival models at tree nodes. This parameter ensures that the fitted coefficients of the survival models are stable. By default this parameter is set to  $10^5$ .

These two new control parameters enforce reliability of the fitted survival models at all nodes, which further produces reliable test statistics that can accurately reflect the relationships between the time-to-event and the longitudinal outcomes.

### 3 Simulation results: time-invariant covariates

In this section, we use simulations to study the behavior of JLCT, and compare JLCT with JLCM. The data are generated such that the time-to-event is correlated with the longitudinal outcomes, but the two are independent conditioning on the latent classes. Thus, the key assumption of conditional independence holds on the simulated data.

We begin with a relatively simple situation where all of the covariates are time-invariant, and thus the time-to-event and latent class memberships are determined by time-invariant covariates. This scenario agrees with the setup of JLCM. In the next section (Section 4) we consider the general scenario where all covariates are time-varying.

The simulation setup varies in the structure of latent classes and in the distribution of time-to-event. We consider four structures of latent classes (as functions of covariates  $X_1$  and  $X_2$ ): tree partition, linear separation, non-linear separation, and asymmetric tree partition, which are shown in Figure 1. Class membership for each subject is determined based on an underlying probability vector, with the concentration level  $p_0$  being defined as the probability of falling into the most probable class; see Appendix B.2 for details. We consider three distributions for baseline hazards of time-to-event data: exponential, Weibull with decreasing hazards with time (Weibull-D), and Weibull with increasing hazards with time (Weibull-I). We give a full description of the simulation setup with time-invariant covariates in Appendix B.

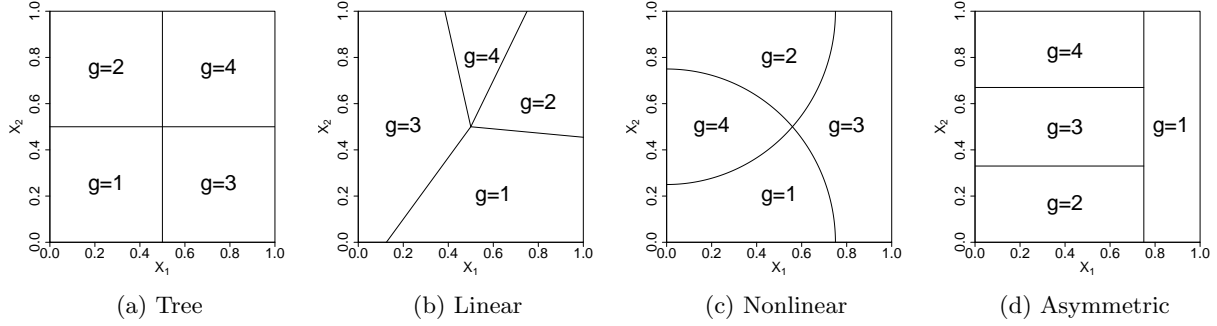


Figure 1: Four structures of latent class membership based on  $X_1$  and  $X_2$ : (a) Tree partition, (b) Linear partition, (c) Nonlinear partition, (d) Asymmetric tree partition.

### 3.1 Methods and measures

We compare four methods on the simulated datasets.

1. A baseline model that treats the entire dataset as one latent class. This is equivalent to JLCT with stopping threshold  $s = \infty$ . After the tree is constructed, we fit a Cox PH model.
2. A JLCT with the stopping threshold  $s = 3.84$ . The tree is pruned to have no more than six terminal nodes, which coincides with the maximal number of latent classes we allow for JLCM. After the tree is constructed, we fit a Cox proportional hazards (PH) model with the same baseline hazard function but different Cox PH slopes across terminal nodes.
3. A JLCT that is the same as the second JLCT, except that both baseline hazard functions and Cox PH slopes differ across terminal nodes.
4. A JLCM, with class-specific slopes and class-specific baseline hazard functions in the survival model. The optimal number of latent classes is chosen from  $\{2, 3, 4, 5, 6\}$  using BIC.

All JLCT methods fit the linear mixed-effects model (1) to the longitudinal outcomes after the tree is constructed, taking the terminal nodes to be the latent classes. Given the fitted JLCT and JLCM, we predict longitudinal outcomes and time-to-event (in terms of survival curves) on both in-sample and out-of-sample data. The details of the prediction procedure are given in Appendix B.5.

We measure performance of the four methods by prediction accuracy (both in-sample and out-of-sample), and by the difference between fitted and true parameters. To compute the out-of-sample measures, at each simulation run we generate a new random sample of  $N$  subjects, using the same data generating process for the in-sample data. We consider the following measures:

- The integrated squared error (ISE) measures the accuracy of the predicted survival curve. The ISE is defined as follows for a set of  $N$  subjects :

$$\text{ISE} = \frac{1}{N} \sum_{i=1}^N \frac{1}{\max_i T_i} \int_0^{\max_i T_i} (\hat{S}_i(t) - S_i(t))^2 dt,$$

where  $\hat{S}_i(t)$  and  $S_i(t)$  are the predicted and the true survival probability for subject  $i$  at time  $t$ , respectively. We compute ISE on in-sample subjects ( $\text{ISE}_{\text{in}}$ ) and on out-of-sample subjects ( $\text{ISE}_{\text{out}}$ ).

- $\text{MSE}_y$  measures the accuracy of longitudinal prediction, which is defined for a set of  $N$  subjects with  $\sum_{i=1}^N n_i$  longitudinal outcomes:

$$\text{MSE}_y = \frac{1}{\sum_{i=1}^N n_i} \sum_{i=1}^N \sum_{j=1}^{n_i} (\hat{y}_{ij} - y_{ij})^2,$$

where we denote by  $\hat{y}_{ij}$  and  $y_{ij}$  the predicted and the true  $j$ -th longitudinal outcome of subject  $i$ , respectively. We compute  $\text{MSE}_y$  on in-sample subjects ( $\text{MSE}_{y_{\text{in}}}$ ) and on out-of-sample subjects ( $\text{MSE}_{y_{\text{out}}}$ ).

- $\text{MSE}_b$  measures the difference between the estimated and the true Cox PH slope coefficients, on a set of  $N$  subjects with  $\sum_{i=1}^N n_i$  observations:

$$\text{MSE}_b = \frac{1}{\sum_{i=1}^N n_i} \sum_{i=1}^N \sum_{j=1}^{n_i} \left\| \hat{\mathbf{b}}_{\hat{d}_{ij}} - \mathbf{b}_{g_{ij}} \right\|_2^2,$$

where  $\hat{\mathbf{b}}_k$  and  $\mathbf{b}_k$  are the estimated and the true Cox PH slopes for latent class  $k$ , and where  $\hat{d}_{ij}$  and  $g_{ij}$  are the predicted and the true latent class membership for the  $j$ -th observation of subject  $i$ , respectively.

It is worth emphasizing that JLCM uses extra information, such as the longitudinal outcomes and time-to-event, to predict latent class membership for in-sample subjects. The quality of latent class membership prediction directly affects that of time-to-event and longitudinal outcomes predictions, and thus JLCM is advantaged compared to JLCT for in-sample performance. A comparison between the two is only fair on out-of-sample subjects, since the longitudinal outcomes and time-to-event are no longer available to JLCM at prediction time, and therefore the two methods use the same amount of information for prediction. In view of this, we focus on comparing the out-of-sample measures in this section, and present the in-sample prediction results in Appendix D.

### 3.2 Results

Figures 2a to 2c show the boxplots of  $\text{ISE}_{\text{out}}$ ,  $\text{MSE}_{y_{\text{out}}}$ , and  $\text{MSE}_b$  respectively, on  $\log_{10}$  scale for  $N = 500$ , light censoring, and Weibull-I distributions, for 16 combinations of latent class structure and concentration level:  $\{\text{Tree, Linear, Nonlinear, Asymmetric}\} \times \{p_0 = 0.5, p_0 = 0.7, p_0 = 0.85, p_0 = 1\}$ . The experiments are repeated 100 times for JLCT, and 20 times for JLCM under each setting. (Since JLCM is prohibitively time-consuming, we only perform 20 runs per setting.) We only consider large concentration levels  $p_0 \geq 0.5$ , where the majority class of a particular subject is dominating the remaining classes in probability that the subject will actually be a member of that class. The results for other baseline hazard distributions and performance measures are given in Appendix D.

Figure 2a shows that the accuracies of survival predictions of JLCT (Methods 2 & 3) and JLCM (Method 4) are comparable, with JLCT being slightly worse, under the settings where latent classes are generated from probabilistic models ( $p_0 < 1$ ). In particular, when the latent class structure comes from a linear separation (Linear) and therefore the simulated data matches exactly the model of JLCM, JLCT still performs comparably to JLCM (e.g.  $p_0 = 0.85$ , “Linear”). The gap between JLCT and JLCM decreases as the concentration level increases from  $p_0 = 0.25$  to 1. In the case where  $p_0 = 1$  and thus latent classes are generated by a deterministic partitioning, JLCT is more effective than JLCM in all settings except nonlinear partitioning. In particular, when the latent class model follows the deterministic partitioning by a tree ( $p_0 = 1$ , “Tree”) and thus matches the model of JLCT, JLCT outperforms JLCM by a significant margin. Furthermore, JLCM tends to have higher variance in ISE values, due to occasionally unconverged JLCM runs.

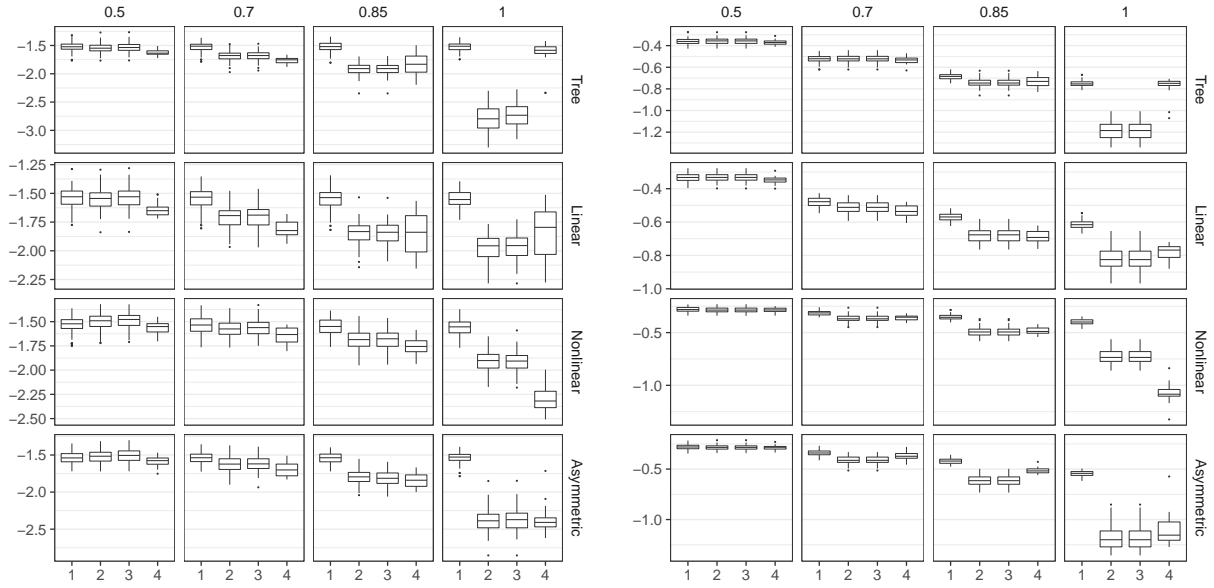
A similar pattern appears for  $\text{MSE}_{y_{\text{out}}}$  in Figure 2b, with JLCT and JLCM comparable for most settings, and JLCT significantly outperforming JLCM when the simulated data come from the underlying model of JLCT. Regarding estimation accuracy of Cox PH slopes (Figure 2c), the same pattern shows up here as well, although there exist more outliers in all methods.

Methods 2 and 3 give very similar results. Indeed, the constructed JLCT trees of the two methods coincide, and only the survival models that are fitted afterwards differ. Method 2 assumes a single baseline hazard function shared across terminal nodes, which agrees with the true data generating scheme. Nevertheless, Methods 2 and 3 have almost identical out-of-sample performances ( $\text{ISE}_{\text{out}}$  and  $\text{MSE}_{y_{\text{out}}}$ ), which suggests that introducing additional parameters for node-specific baseline hazard functions does not hurt the prediction performance for the simulated data. In practice, it is often unclear whether the latent classes share a single baseline hazard function. Our results suggest that in such a case, we can assume a separate baseline hazard function for each terminal node, without worrying about over-fitting the data. In later simulations and real application, we only consider the Cox PH model with separate baseline hazard functions across terminal nodes.

Table 1 shows the average running time of JLCT (over 100 runs) and JLCM (over 20 runs) under the same settings as the plots. The running time of JLCT includes constructing the tree and fitting the two survival models of Methods 2 and 3. The running time of JLCM includes fitting with all numbers of latent classes  $g \in \{2, 3, 4, 5, 6\}$ . Clearly, JLCT is orders of magnitude faster than JLCM across all settings: JLCT completes one run within a minute, while JLCM typically takes 25 to 45 minutes. The

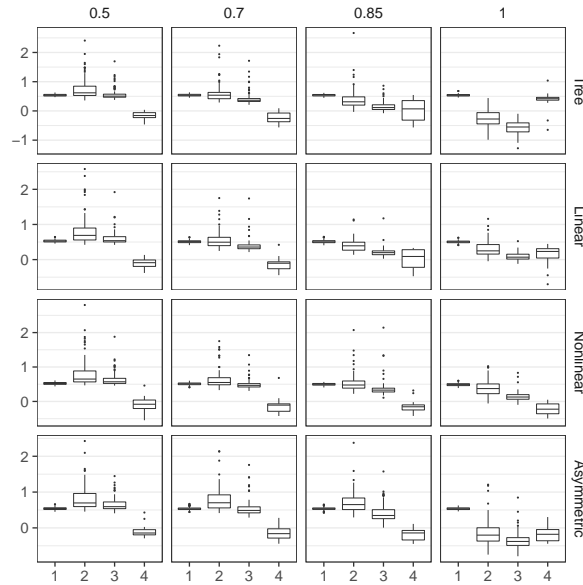
running time for other censoring levels and baseline hazard distributions are similar. All of the simulations (including those in Section 4) are performed on high performance computing nodes with 3.0GHz CPU and 62 GB of memory.

The simulation results demonstrate that when all covariates are time-invariant, which satisfies the assumptions of JLCM, JLCT is comparable to JLCM in prediction performance under most simulation settings. Furthermore, as the latent class membership model approaches a deterministic partitioning, JLCT can significantly outperform JLCM in certain settings. More importantly, JLCT takes much less time to fit, which enables fast model selection for even better performance. In the next section, we study the scenario where all covariates are time-varying, and thus JLCM does not apply directly, and demonstrate that JLCT gains additional advantage over JLCM by fully exploiting the time-varying nature of the data.



(a)  $ISE_{out}$

(b)  $MSE_{y_{out}}$



(c)  $MSE_b$

Figure 2: Boxplots of prediction performance, on  $\log_{10}$  scale. The simulation only uses time-invariant covariates, with  $N = 500$ , light censoring and Weibull-I distribution. Each panel contains four methods: (1) JLCT with no split, (2) JLCT with same baseline hazard function but different Cox PH slopes across latent classes, (3) JLCT with different baseline hazard functions and different Cox PH slopes across latent classes, (4) JLCM with different baseline hazard functions and different Cox PH slopes across latent classes, using an interaction term in modeling latent class membership.



Table 1: The average running time in seconds (standard deviation in parentheses) on a dataset with time-invariant covariates,  $N = 500$ , light censoring, and Weibull-I distribution.

Structure	$p_0$	JLCT	JLCM
Tree	0.5	34.37 (2.45)	1853.02 (301.94)
	0.7	28.27 (2.22)	2151.44 (426.60)
	0.85	19.16 (1.92)	1921.36 (381.52)
	1	9.66 (0.46)	1691.30 (261.07)
Linear	0.5	46.48 (3.91)	1674.99 (136.63)
	0.7	38.86 (3.43)	2170.75 (369.54)
	0.85	28.62 (2.80)	1826.12 (510.56)
	1	30.97 (3.79)	1794.20 (369.24)
Nonlinear	0.5	36.74 (3.09)	1565.98 (368.03)
	0.7	28.68 (2.41)	1627.64 (260.65)
	0.85	31.02 (2.75)	1744.02 (251.78)
	1	19.50 (2.60)	3302.90 (358.73)
Asymmetric	0.5	35.26 (2.61)	1555.53 (382.61)
	0.7	31.46 (2.64)	1680.21 (309.16)
	0.85	22.99 (2.90)	1781.39 (196.74)
	1	9.62 (1.26)	2757.40 (627.39)

## 4 Simulation results: time-varying covariates

In this section, we compare JLCT with JLCM under the general scenario where all covariates are time-varying. JLCT can work with time-varying covariates in a straightforward way, but JLCM can only use a subset of available time-varying data, which limits its prediction performance.

The setup greatly resembles that of the time-invariant scenario in Section 3, except that all covariates are now time-varying. As a result, subject  $i$  might change from one latent class to another at time  $t_i$ , which directly affects the generation of longitudinal outcomes and time-to-event. In Appendix C we give a full description of the setup with time-varying covariates.

### 4.1 Methods and measures

Given the simulated data, JLCT and JLCM use the same choice of covariates in each modeling component ( $\mathbf{X}^s, \mathbf{X}^f, \mathbf{X}^r, \mathbf{X}^g$ ) as in the time-invariant scenario. We can directly fit JLCT to the simulated data using the time-varying covariates. On the other hand, JLCM does not support time-varying covariates in either the latent class membership model or the time-to-event model. If a time-varying covariate is used in either model, by default JLCM will take the first encountered value of each subject and use it as if the covariate is time-invariant; that is, it takes the value as a baseline value and uses that. We denote by  $\mathbf{X}_i^s|_{1st}$  and  $\mathbf{X}_i^g|_{1st}$  the first encountered values of the time-varying covariates  $\mathbf{X}_i^s$  and  $\mathbf{X}_i^g$ . Thus we can still fit JLCM to the simulated data, but JLCM automatically replaces  $\mathbf{X}^s, \mathbf{X}^g$  with  $\mathbf{X}^s|_{1st}, \mathbf{X}^g|_{1st}$ .

Since JLCM only uses the first encountered values per subject for covariates  $\mathbf{X}^s, \mathbf{X}^g$ , it is not clear whether differences in performance of JLCM and JLCT are due to the additional information contained in later values of time-varying covariates, or because of the difference in the methodology itself. For the purpose of decomposing the difference, we also examine a version of JLCT that is restricted to using  $\mathbf{X}^s|_{1st}$  and  $\mathbf{X}^g|_{1st}$ . To summarize, we fit the following five methods to the simulated data:

1. A baseline model that treats the entire dataset as one latent class. This is equivalent to JLCT with stopping threshold  $s = \infty$ .
2. A JLCT model, using converted time-invariant covariates  $\mathbf{X}^g|_{1st}$  and  $\mathbf{X}^s|_{1st}$  to model latent class and time-to-event, while using  $\mathbf{X}^f, \mathbf{X}^r$  to model longitudinal outcomes.
3. A JLCT model, using converted time-invariant covariates  $\mathbf{X}^g|_{1st}$  to model latent class, while using  $\mathbf{X}^s, \mathbf{X}^f, \mathbf{X}^r$  to model time-to-event and longitudinal outcomes.
4. A JLCT model, using original time-varying covariates  $\mathbf{X}^g, \mathbf{X}^s, \mathbf{X}^f, \mathbf{X}^r$  for all of the modeling components. This is the default JLCT.

5. JLCM, using converted time-invariant covariates  $\mathbf{X}^g|_{1st}$  and  $\mathbf{X}^s|_{1st}$  to model latent class and time-to-event, meanwhile using  $\mathbf{X}^f, \mathbf{X}^r$  to model longitudinal outcomes. This is the default JLCM, and it uses the same amount of information as the second JLCT (Method 2). In JLCM, we allow class-specific coefficients for  $\mathbf{X}^s$  in the survival model, as well as class-specific Weibull baseline risk functions. The optimal number of latent classes is chosen from  $\{2, 3, 4, 5, 6\}$  using BIC.

All JLCT models use stopping threshold 3.84 and are pruned to have no more than 6 terminal nodes. Once a tree is constructed, we fit an extended Cox model with different hazard functions and different slopes across terminal nodes. We use the same prediction procedure and performance measures as in the time-invariant scenario to compare these five methods.

## 4.2 Results

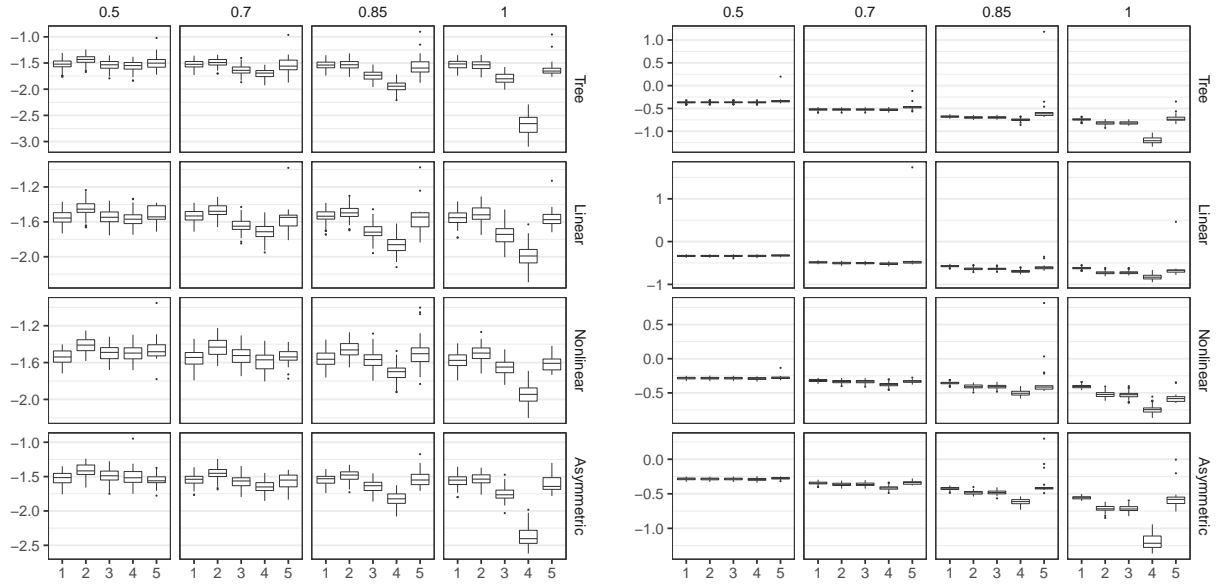
Figures 3a to 3c show the boxplots of  $ISE_{out}$ ,  $MSE_{y_{out}}$ , and  $MSE_b$  respectively, on  $\log_{10}$  scale for  $N = 500$ , light censoring, and Weibull-I distributions, for 16 combinations of latent class structure and concentration level:  $\{\text{Tree, Linear, Nonlinear, Asymmetric}\} \times \{p_0 = 0.5, p_0 = 0.7, p_0 = 0.85, p_0 = 1\}$ . The experiments are repeated 100 times for JLCT, and 20 times for JLCM under each setting. The results for other baseline hazards distributions and performance measures are given in Appendix E.

Figure 3a demonstrates a clear decomposition of the differences in ISE between JLCT and JLCM. The first JLCT method with no split serves as a benchmark. The second JLCT method uses the converted “time-invariant” (baseline) data, and it has slightly larger ISE values than JLCM (Method 5), which uses the same converted data. If we allow JLCT to use the original time-varying covariates in the survival model (Method 3), then the ISE becomes smaller than that of JLCM. This demonstrates the potential of time-varying covariates in making accurate survival predictions. When we further allow JLCT to use the original time-varying covariates in the class membership model as well (Method 4), the ISE decreases even more and becomes significantly better than that of JLCM. That is, if each subject is allowed to switch between latent classes throughout the time of study, and the estimated membership is also allowed to switch, we can achieve additional improvement in survival predictions when such switching actually occurs in the population.

The ISE of the default JLCT (Method 4) improves when the latent class membership becomes less noisy, i.e.  $p_0$  increases, and JLCT is much more favorable than JLCM when the latent classes are generated by a nearly deterministic partitioning ( $p_0 \geq 0.85$ ). In particular, when the partitioning is deterministic ( $p_0 = 1$ ) and the underlying structure is a tree (Tree, and Asymmetric Tree), JLCT is expected to perform well since data are generated according to its underlying model, and does indeed outperform JLCM by a much larger margin in deterministic tree setups.

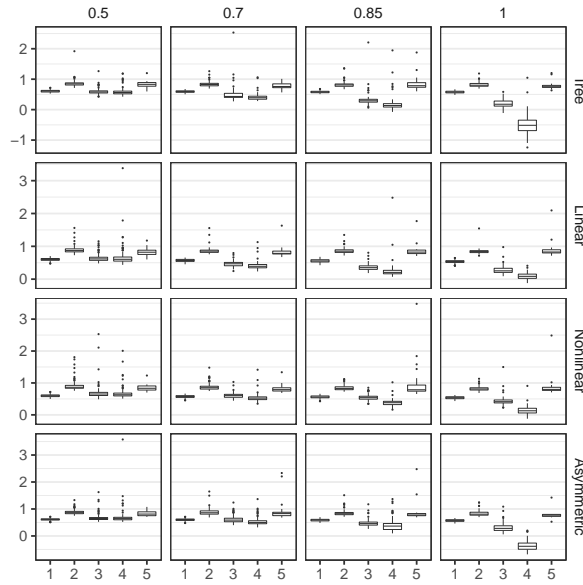
Similar patterns appear in  $MSE_{y_{out}}$  (Figure 3b), and  $MSE_b$  (Figure 3c), where the default JLCT (Method 4) outperforms all other methods when the concentration level is reasonably large ( $p_0 \geq 0.85$ ). The other two measures have less variability relative to overall levels than does ISE.

We report average running times of the default JLCT (Method 4) and JLCM (Method 5) in Table 2. The running times of all three JLCT methods (Methods 2 to 4) are comparable, thus we only keep the default JLCT (Method 4) in our comparison. Table 2 shows again that JLCT is orders of magnitude faster than JLCM. Compared to the time-invariant scenario (Table 1), the change in JLCT’s running time is negligible, while JLCM takes much longer to run. This observation is surprising, since internally JLCM still fits a time-invariant dataset. The longer running time of JLCM suggests that the data generated by time-varying covariates contain more complex signals, which results in longer running times in fitting the (incorrect) JLCM model.



(a)  $ISE_{out}$

(b)  $MSE_{y_{out}}$



(c)  $MSE_b$

Figure 3: Boxplots of prediction performance, on  $\log_{10}$  scale. The simulation uses time-varying covariates, with  $N = 500$ , light censoring, and Weibull-I distribution. Each panel contains five methods: (1) JLCT with no split, and using time-varying survival covariates, (2) JLCT with “time-invariant” latent class and survival covariates, (3) JLCT with “time-invariant” latent class covariates and time-varying survival covariates, (4) JLCT with time-varying latent class and survival covariates, (5) JLCM with “time-invariant” latent class and survival covariates.

Table 2: The average running time in seconds (standard deviation in parentheses) on a dataset with time-varying covariates,  $N = 500$ , light censoring and Weibull-I distribution.

Structure	$p_0$	JLCT	JLCM
Tree	0.5	42.66 (2.43)	1928.86 (506.13)
	0.7	33.92 (4.33)	1863.05 (481.95)
	0.85	20.62 (3.04)	2037.55 (564.91)
	1	7.96 (0.58)	2189.12 (468.41)
Linear	0.5	54.18 (4.75)	2109.98 (313.72)
	0.7	42.78 (3.24)	2114.97 (479.38)
	0.85	35.23 (4.21)	2140.96 (269.62)
	1	27.97 (3.83)	2366.95 (718.97)
Nonlinear	0.5	40.54 (4.86)	2044.40 (201.28)
	0.7	33.25 (3.09)	2142.03 (177.44)
	0.85	30.70 (6.02)	2150.83 (249.17)
	1	18.87 (2.72)	2175.97 (455.68)
Asymmetric	0.5	40.60 (5.31)	2154.53 (240.17)
	0.7	32.34 (2.47)	2219.78 (207.58)
	0.85	25.59 (3.06)	2233.15 (219.98)
	1	7.00 (1.05)	2165.21 (43.30)

## 5 Application

In this section, we apply JLCT to a real dataset, the PAQUID dataset, which was also examined in [Proust-Lima et al. \[2017\]](#), and compare its performance to that of JLCM.

We use the PAQUID (Personnes Agees Quid) dataset from the R package `lcm`. The provided PAQUID dataset consists of 2250 records of 500 subjects from the PAQUID study [\[Letenneur et al., 1994\]](#). The PAQUID dataset collects five time-varying values (`MMSE`, `IST`, `BVRT`, `HIER`, `CESD`) along with age at visit (`age`). The event in the dataset is the dementia diagnosis (`dem`), and the time-to-event is the age at dementia diagnosis or last visit, `agedem`. The PAQUID dataset also collects three time-invariant covariates: education (`CEP`), gender (`male`), and age at the entry of the study (`age_init`). As suggested by [Proust-Lima et al. \[2017\]](#), we normalize the highly asymmetric covariate `MMSE` and only consider its normalized version `normMMSE`; we also construct a new covariate `age65 = (age - 65)/10`. Our goal for this dataset is to jointly model the trajectories of `normMMSE` (longitudinal outcomes) and the risk of dementia (time-to-event), using the remaining covariates.

We consider two JLCM and three JLCT models:

1. (JLCM<sub>1</sub>) We adopt the time-invariant JLCM model in [Proust-Lima et al. \[2017\]](#): The trajectories of `normMMSE` depend on fixed effects  $\mathbf{X}^f = \{\text{age65}, \text{age65}^2, \text{CEP}, \text{male}\}$ , and random effects  $\mathbf{X}^r = \{\text{age65}, \text{age65}^2\}$ . The risk of dementia depends on  $\mathbf{X}^s = \{\text{CEP}, \text{male}\}$ , with class-specific Weibull baseline hazards function. The class membership is modeled by  $\mathbf{X}^g = \{\text{CEP}, \text{male}\}$ .
2. (JLCM<sub>2</sub>) We extend JLCM<sub>1</sub> to using additional covariates: the survival model uses covariates  $\mathbf{X}^s = \{\text{CEP}, \text{male}, \text{age\_init}, \text{BVRT}|_{1\text{st}}, \text{IST}|_{1\text{st}}, \text{HIER}|_{1\text{st}}, \text{CESD}|_{1\text{st}}\}$ ; the class membership model uses covariates  $\mathbf{X}^g = \{\text{CEP}, \text{male}, \text{age65}|_{1\text{st}}, \text{BVRT}|_{1\text{st}}, \text{IST}|_{1\text{st}}, \text{HIER}|_{1\text{st}}, \text{CESD}|_{1\text{st}}\}$ . The rest of the model remains the same as in the time-invariant JLCM<sub>1</sub>. Note that JLCM automatically uses the first encountered value  $X|_{1\text{st}}$  of any time-varying covariate  $X$ .
3. (JLCT<sub>1</sub>) The first JLCT model uses the same sets of covariates as JLCM<sub>1</sub>.
4. (JLCT<sub>2</sub>) The second JLCT model uses the same sets of covariates as JLCM<sub>2</sub>. In particular, JLCT<sub>2</sub> also uses  $X|_{1\text{st}}$  for any time-varying covariate  $X$ .
5. (JLCT<sub>3</sub>) The last JLCT model adopts the same sets of covariates as JLCM<sub>2</sub>, but using the original values of any time-varying covariate:  $\mathbf{X}^s = \{\text{CEP}, \text{male}, \text{age\_init}, \text{BVRT}, \text{IST}, \text{HIER}, \text{CESD}\}$ ; and  $\mathbf{X}^g = \{\text{CEP}, \text{male}, \text{age65}, \text{BVRT}, \text{IST}, \text{HIER}, \text{CESD}\}$ . The rest of the model remains the same as in the time-invariant JLCM<sub>2</sub>. JLCT<sub>3</sub> is our main model with no comparable competitors.

For the two JLCM models, the number of latent classes is chosen from 2 to 6 according to the BIC selection criterion. For the three JLCT models, we set the stopping threshold to 3.84 and prune the trees

Table 3: Performance of JLCM and JLCT methods on the PAQUID dataset.

	JLCM <sub>1</sub>	JLCM <sub>2</sub>	JLCT <sub>1</sub>	JLCT <sub>2</sub>	JLCT <sub>3</sub>
IBS	0.1731	0.4467	0.1611	0.169	0.0966
RMSE	14.7588	18.3544	14.5503	14.2912	14.5014
Time (secs)	2448.7026	4107.6193	1.6998	40.9126	87.9072

to have no more than 6 terminal nodes. The survival models of all five methods assume class-specific baseline hazards functions and the same slope coefficients across classes, which is adopted by Proust-Lima et al. [2017].

We use the root mean squared error (RMSE) to measure the accuracy of the predicted longitudinal outcomes. To evaluate the accuracy of the time-to-event predictions, we take the commonly used measure, the Brier score and its integrated version, IBS [Graf et al., 1999]. The Brier score (BS) at a fixed time  $t$  is defined as

$$BS(t) = \frac{1}{N} \sum_{i=1}^N \left( I(Y_i > t) - \widehat{S}(t|X_i) \right)^2,$$

where  $\widehat{S}(t|X_i)$  is the predicted probability of survival at time  $t$  conditioning on subject  $i$ 's predictor vector  $X_i$ , and  $Y_i$  is the time-to-event of subject  $i$ . The Integrated Brier score (IBS) is therefore defined as

$$IBS = \frac{1}{\max Y_i} \int_0^{\max Y_i} BS(Y) dY.$$

We compute the accuracy measure on out-of-sample subjects using 10-fold cross-validation as follows. We first randomly divide the dataset into 10 folds of equal size, where we take care such that observations of a single subject belong to the same fold. Next, we hold out one fold of data and run the model on the remaining nine folds. The performance of the model is then evaluated on the held out data. The procedure is repeated 10 times, where each of the 10 folds is used for out-of-sample evaluation.

We report the average prediction measure and running time over the 10 folds in Table 3. When using only time-invariant covariates, JLCT<sub>1</sub> performs similarly to its counterpart JLCM<sub>1</sub> in prediction accuracy (IBS and RMSE). By adding four ‘‘time-invariant’’ covariates (which are converted from time-varying ones) to the class membership and survival models, the performance of JLCT<sub>2</sub> remains similar, but the performance of JLCM<sub>2</sub> becomes much worse, mainly because JLCM failed to converge when optimizing the log-likelihood function. When using the original time-varying covariates in the class membership and survival models, however, JLCT<sub>3</sub> improves its time-to-event prediction accuracy and outperforms all other methods by a significant margin on that measure. When we look at the running time, JLCT is much faster than JLCM: fitting using JLCT took no more than 2 minutes even for the most complex model (JLCT<sub>3</sub>), while fitting using JLCM took from 40 to 60 minutes. The experiments are performed on a desktop with 2.26GHz CPU and 32GB of memory.

The results in Table 3 demonstrate two key advantages of the tree-based approach JLCT over the parametric JLCM: JLCT is capable of providing significantly better prediction performance with the use of time-varying covariates in all of its modeling components, and it can be orders of magnitude faster to fit JLCT than to fit JLCM.

Figures 4a, 4b, and 4c give the JLCT tree structure from JLCT<sub>1</sub>, JLCT<sub>2</sub> and JLCT<sub>3</sub> respectively, which are fit using the entire PAQUID dataset. The numbers in each box display the test statistics TS, and the proportion of observations contained in the current node. We make the following observations:

- When fitting with only time-invariant covariates CEP and male, JLCT<sub>1</sub> first splits into CEP= 0 and CEP= 1, then splits on gender within the node of CEP = 1. Two of the three terminal nodes have final TS greater than the stopping criterion, 3.84, which indicates potential association between longitudinal and survival data within these two nodes. However, since CEP and male take binary values {0, 1}, JLCT<sub>1</sub> cannot split further. Thus, it seems unlikely that using only time-invariant covariates provides adequate fit for these data.
- JLCT<sub>2</sub> uses more splitting covariates,  $\mathbf{X}^{\mathcal{E}} = \{\text{CEP, male, age65}|_{1st}, \text{BVRT}|_{1st}, \text{IST}|_{1st}, \text{HIER}|_{1st}, \text{CESD}|_{1st}\}$ , with some of the covariates converted from time-varying ones. JLCT<sub>2</sub> makes multiple splits on CESD|<sub>1st</sub>, and then makes a final split on ISE|<sub>1st</sub>. With additional covariates to split on, JLCT<sub>2</sub> ends up with five terminal nodes, each having a test statistic less than 3.84, and thus JLCT<sub>2</sub> has uncovered a good partitioning in the sense that the terminal nodes lack evidence of association between longitudinal and survival outcomes. However, the prediction performance of JLCT<sub>2</sub> shows

no significant improvement over  $\text{JLCT}_1$  based on cross-validation, suggesting that the JLCT models have reached a limit with only time-invariant covariates to use.

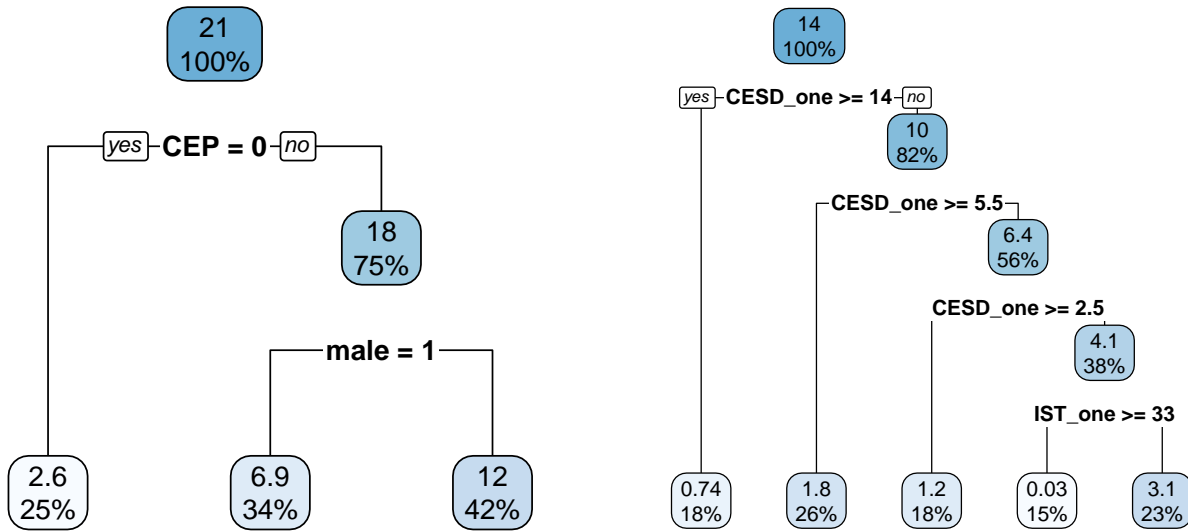
- $\text{JLCT}_3$  uses the original time-varying values of the  $\mathbf{X}^{\text{S}}$  covariates in  $\text{JLCT}_2$ . The tree splits into three nodes based only on **age** (splitting at ages 82 and 90), suggesting that people transition into different dementia statuses as they get older, which are reflected in both cognitive test score (**normMMSE**) and time until a dementia diagnosis. Furthermore, all three nodes obtain a final test statistic less than 3.84, which indicates a good partitioning of the population in terms of preserving conditional independence within groups. Finally, with time-varying latent class memberships and time-varying covariates in the survival models,  $\text{JLCT}_3$  achieves significant improvement in prediction performance of time to dementia diagnosis.

## 6 Conclusion

In this paper, we have proposed a tree-based approach (JLCT) to jointly model longitudinal outcomes and time-to-event with latent classes. Simulations and real application on the PAQUID dataset show that when covariates are time-invariant, JLCT performs comparably to the common parametric joint latent class modeling approach JLCM. When the covariates become time-varying, JLCT makes full use of the time-varying information and can demonstrate significant advantage over JLCM, which can only use a subset of the available time-varying data. In addition, JLCT is orders of magnitude faster than JLCM under both scenarios.

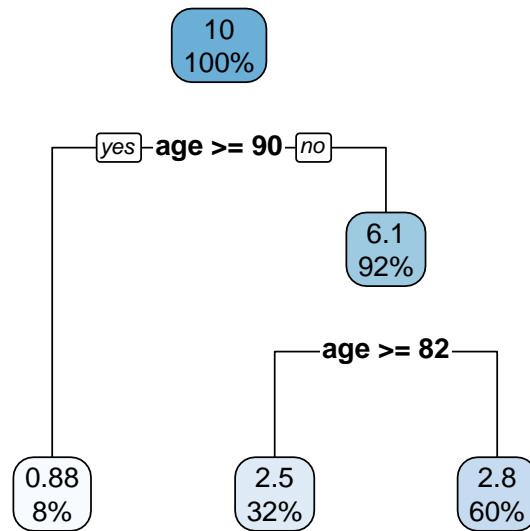
There are several interesting extensions of the JLCT method that could be explored. The PAQUID data set discussed in [Proust-Lima et al. \[2017\]](#) and in Section 5 is actually one exhibiting competing risks, since there is a risk of death before dementia is exhibited, but this was ignored in the analysis. It would be of interest to generalize JLCT to account for this. Often survival values are only known to within an interval of time (interval-censoring), and JLCT could be adapted to that situation as well. In addition, the analysis here only allows for one longitudinal outcome, but sometimes several biomarkers are available for a patient, and it would be useful to generalize JLCT to allow for that.

An R package, `jlctree`, that implements JLCT is available at CRAN. Appendix F provides code illustrating its use.



(a) JLCT<sub>1</sub> tree structure.

(b) JLCT<sub>2</sub> tree structure.



(c) JLCT<sub>3</sub> tree structure.

Figure 4: The tree structures returned by JLCT methods. JLCT<sub>1</sub>: constructed with  $\mathbf{X}^g = \{\text{CEP}, \text{male}\}$ . JLCT<sub>2</sub>: constructed with  $\mathbf{X}^g = \{\text{CEP}, \text{male}, \text{age65}|_{1st}, \text{BVRT}|_{1st}, \text{IST}|_{1st}, \text{HIER}|_{1st}, \text{CESD}|_{1st}\}$ . JLCT<sub>3</sub>: constructed with  $\mathbf{X}^g = \{\text{CEP}, \text{male}, \text{age}, \text{BVRT}, \text{IST}, \text{HIER}, \text{CESD}\}$ .

## References

- P. K. Andersen and R. D. Gill. Cox's regression model for counting processes: A large sample study. *The Annals of Statistics*, 10(4):1100–1120, 1982.
- D. Bates, M. Mächler, B. Bolker, and S. Walker. Fitting linear mixed-effects models using lme4. *Journal of Statistical Software*, 67(1):1–48, 2015.
- L. Breiman, J. H. Friedman, R. A. Olshen, and C. J. Stone. *Classification and Regression Trees*.

- Wadsworth and Brooks, Monterey, CA, USA, 1984.
- D. R. Cox. Regression models and life-tables. *Journal of the Royal Statistical Society. Series B*, 34(2): 187–220, 1972.
- J. Crowley and M. Hu. Covariance analysis of heart transplant survival data. *Journal of the American Statistical Association*, 72(357):27–36, 1977.
- F. W. Dekker, R. De Mutsert, P. C. Van Dijk, C. Zoccali, and K. J. Jager. Survival analysis: Time-dependent effects and time-varying risk factors. *Kidney International*, 74(8):994–997, 2008.
- R. Dicker, F. Coronado, D. Koo, and R. G. Parrish. Principles of epidemiology in public health practice. *US Department of Health and Human Services*, 2006.
- W. Fu and J. S. Simonoff. Survival trees for left-truncated and right-censored data, with application to time-varying covariate data. *Biostatistics*, 18(2):352–369, 2017.
- F. G. Garre, A. H. Zwinderman, R. B. Geskus, and Y. W. Sijpkens. A joint latent class changepoint model to improve the prediction of time to graft failure. *Journal of the Royal Statistical Society: Series A*, 171(1):299–308, 2008.
- E. Graf, C. Schmoor, W. Sauerbrei, and M. Schumacher. Assessment and comparison of prognostic classification schemes for survival data. *Statistics in Medicine*, 18(17-18):2529–2545, 1999.
- T. Hajiro, K. Nishimura, M. Tsukino, A. Ikeda, and T. Oga. Stages of disease severity and factors that affect the health status of patients with chronic obstructive pulmonary disease. *Respiratory Medicine*, 94(9):841–846, 2000.
- T. Hastie, R. Tibshirani, and J. Friedman. *The Elements of Statistical Learning*. Springer Series in Statistics. Springer New York Inc., New York, NY, USA, 2001.
- R. Henderson, P. Diggle, and A. Dobson. Joint modelling of longitudinal measurements and event time data. *Biostatistics*, 1(4):465–480, 2000.
- I. P. Jongerden, B. Speelberg, C. L. Satizábal, A. G. Buiting, M. A. Leverstein-van Hall, J. Kesecioglu, and M. J. Bonten. The role of systemic antibiotics in acquiring respiratory tract colonization with gram-negative bacteria in intensive care patients: A nested cohort study. *Critical Care Medicine*, 43(4):774–780, 2015.
- C. P. Kovesdy, J. E. Anderson, and K. Kalantar-Zadeh. Paradoxical association between body mass index and mortality in men with CKD not yet on dialysis. *American Journal of Kidney Diseases*, 49(5):581–591, 2007.
- N. M. Laird and J. H. Ware. Random-effects models for longitudinal data. *Biometrics*, 38(4):963–974, 1982.
- L. Letenneur, D. Commenges, J.-F. Dartigues, and P. Barberger-Gateau. Incidence of dementia and Alzheimer’s disease in elderly community residents of south-western France. *International Journal of Epidemiology*, 23(6):1256–1261, 1994.
- H. Lin, B. W. Turnbull, C. E. McCulloch, and E. H. Slate. Latent class models for joint analysis of longitudinal biomarker and event process data: Application to longitudinal prostate-specific antigen readings and prostate cancer. *Journal of the American Statistical Association*, 97(457):53–65, 2002.
- L. S. Munoz-Price, J. F. Frencken, S. Tarima, and M. Bonten. Handling time-dependent variables: Antibiotics and antibiotic resistance. *Clinical Infectious Diseases*, 62(12):1558–1563, 2016.
- C. Proust-Lima and J. M. Taylor. Development and validation of a dynamic prognostic tool for prostate cancer recurrence using repeated measures of posttreatment PSA: A joint modeling approach. *Biostatistics*, 10(3):535–549, 2009.
- C. Proust-Lima, P. Joly, J.-F. Dartigues, and H. Jacqmin-Gadda. Joint modelling of multivariate longitudinal outcomes and a time-to-event: A nonlinear latent class approach. *Computational Statistics & Data Analysis*, 53(4):1142–1154, 2009.



- C. Proust-Lima, M. Séne, J. M. Taylor, and H. Jacqmin-Gadda. Joint latent class models for longitudinal and time-to-event data: A review. *Statistical Methods in Medical Research*, 23(1):74–90, 2014.
- C. Proust-Lima, V. Philipps, and B. Lique. Estimation of extended mixed models using latent classes and latent processes: The R package lcmm. *Journal of Statistical Software*, 78(2):1–56, 2017.
- C. Proust-Lima, V. Philipps, A. Diakite, and B. Lique. *lcmm: Extended Mixed Models Using Latent Classes and Latent Processes*, 2018. URL <https://cran.r-project.org/package=lcmm>. R package version: 1.7.9.
- D. Rizopoulos. JM: An R package for the joint modelling of longitudinal and time-to-event data. *Journal of Statistical Software*, 35(9):1–33, 2010.
- T. M. Therneau. *A Package for Survival Analysis in S*, 2015. URL <https://CRAN.R-project.org/package=survival>. version 2.38.
- T. M. Therneau and P. M. Grambsch. *Modeling Survival Data: Extending the Cox Model*. Springer, New York, 2000. ISBN 0-387-98784-3.
- A. A. Tsiatis and M. Davidian. Joint modeling of longitudinal and time-to-event data: An overview. *Statistica Sinica*, 14(3):809–834, 2004.
- A. A. Tsiatis, V. Degruittola, and M. S. Wulfsohn. Modeling the relationship of survival to longitudinal data measured with error. Applications to survival and CD4 counts in patients with AIDS. *Journal of the American Statistical Association*, 90(429):27–37, 1995.
- M. S. Wulfsohn and A. A. Tsiatis. A joint model for survival and longitudinal data measured with error. *Biometrics*, 53(1):330–339, 1997.

## A Joint Latent Class Models (JLCM)

In this section, we give a brief introduction to JLCM, and discuss its strengths and weaknesses. More details about JLCM can be found in [Proust-Lima et al. \[2014\]](#).

In JLCM, the latent class membership  $g_i \in \{1, \dots, G\}$  for subject  $i$  is determined by the set of covariates  $\mathbf{X}_i^g$ ; ( $\mathbf{X}_{it}^g$  must be time-invariant in JLCM, so we drop the time indicator  $t$ ), through the following probabilistic model:

$$\pi_{ig} = \Pr(g_i = g | \mathbf{X}_i^g) = \frac{\exp\{\xi_{0g} + \mathbf{X}_i^g \xi_{1g}\}}{\sum_{l=1}^G \exp\{\xi_{0l} + \mathbf{X}_i^g \xi_{1l}\}},$$

where  $\xi_{0g}, \xi_{1g}$  are class-specific intercept and slope parameters for class  $g = 1, \dots, G$ .

The longitudinal outcomes in JLCM are assumed to follow a slightly different linear mixed-effects model than in (1):

$$y_{it}|g_i=g = \mathbf{X}_{it}^f \boldsymbol{\beta}_g + \mathbf{X}_{it}^r \mathbf{u}_{ig} + \varepsilon_{it}, \quad \mathbf{u}_{ig} = \mathbf{u}_i|g_i=g \sim \mathcal{N}(\boldsymbol{\mu}_g, \mathbf{B}_g), \quad \varepsilon_{it} \sim \mathcal{N}(0, \sigma^2),$$

where  $\boldsymbol{\beta}_g$  is the fixed effect vector for class  $g$ , and  $\mathbf{u}_{ig}$  is the random effect vector for subject  $i$  and class  $g$ . The random effect vector  $\mathbf{u}_{ig}$  is independent across latent classes and subjects, and normally distributed with mean  $\boldsymbol{\mu}_g$  and variance-covariance matrix  $\mathbf{B}_g$ . The errors  $\varepsilon_{it}$  are assumed to be independent and normally distributed with mean 0 and variance  $\sigma^2$ , and independent of all of the random effects as well. Let  $f(\mathbf{Y}_i|g_i = g)$  denote the likelihood of longitudinal outcomes  $\mathbf{Y}_i$  given that subject  $i$  belongs to latent class  $g$ .

The time-to-event  $T_i$  is considered to follow the proportional hazards model with time-invariant covariates  $\mathbf{X}^s$ :

$$h_i(t|g_i = g) = h_{0g}(t; \zeta_g) e^{\mathbf{X}_i^s \eta_g}, \quad (4)$$

where  $\zeta_g$  parameterizes the class-specific baseline hazards  $h_{0g}$ , and  $\eta_g$  is associated with the set of covariates  $\mathbf{X}_i^s$  (we drop the time indicator  $t$  from  $\mathbf{X}_{it}^s$  since it must be time-invariant in JLCM). Let  $S_i(t|g_i = g)$  denote the survival probability at time  $t$  if subject  $i$  belongs to latent class  $g$ . Note that the extended Cox model (2) of JLCT extends the proportional hazards model (4) to allow for time-varying covariates.

Let  $\theta_G = (\xi_{0g}, \xi_{1g}, \boldsymbol{\beta}_g, \mathbf{u}_{ig}, \boldsymbol{\mu}_g, \mathbf{B}_g, \sigma, \zeta_g, \eta_g; g = 1, \dots, G, i = 1, \dots, N)$  be the entire vector of parameters of JLCM. These parameters are estimated together via maximizing the log-likelihood function

$$L(\theta_G) = \sum_{i=1}^N \log \left( \sum_{g=1}^G \pi_{ig} f(\mathbf{Y}_i|g_i = g; \theta_G) h_i(T_i|g_i = g; \theta_G)^{\delta_i} S_i(T_i|g_i = g; \theta_G) \right).$$

The log-likelihood function above uses the assumption that conditioning on the latent class membership ( $g_i$ ), longitudinal outcomes ( $\mathbf{Y}_i$ ) and time-to-event ( $T_i, \delta_i$ ) are independent.

As mentioned in the introduction, the concept of latent class membership is of particular interest in clinical studies. JLCM is designed to give parametric descriptions of subjects' tendency of belonging to each latent class, and therefore JLCM is a suitable model when the true latent class is indeed a random outcome with unknown probabilities for each class. The multinomial logistic regression that JLCM uses is a flexible tool to model these unknown probabilities.

Despite the usefulness of latent classes, JLCM has several weaknesses. First of all, the running time of JLCM does not scale well due to its complicated likelihood function. Simulation results show that the running time of JLCM increases exponentially fast as a function of the number of observations, the number of covariates, and the number of assumed latent classes. Secondly, the modeling of time-to-event in JLCM is restricted to the use of time-invariant covariates. However, time-varying covariates are helpful in modeling the time-to-event, especially when treatment or important covariates change during the study, for instance the patient receives a heart transplant [[Crowley and Hu, 1977](#)], or the longitudinal CD4 counts change during the study of AIDS [[Tsiatis et al., 1995](#)]. Research shows that using time-varying covariates can uncover short-term associations between time-to-event and covariates [[Dekker et al., 2008](#), [Kovesdy et al., 2007](#)], and ignoring the time-varying nature of the covariates will lead to time-dependent bias [[Jongerden et al., 2015](#), [Munoz-Price et al., 2016](#)]. The other restriction of JLCM is that the latent class membership model only uses time-invariant covariates, which implies that the latent class membership of a subject is assumed to be fixed throughout the time of study. However, the stage of a disease of a patient is very likely to change during the course of clinical study, for instance the disease would move from its early stages to its peak, and then move to its resolution. When the goal of

joint modeling is to uncover meaningful clustering of the population that leads to definitions of disease stages, it is important to allow time-varying covariates in the latent class membership model, so that the model reflects this real world situation.

## B Simulation setup: time-invariant covariates

In this section we give details of the data generating scheme in the simulation study of time-invariant covariates only (Sections 3).

At each simulation run, for each subject  $i$  we randomly generate five independent, time-invariant covariates  $X_{i1}, \dots, X_{i5}$ . We assume there are four latent classes  $g = 1, \dots, 4$ , which are determined by covariates  $X_1, X_2$ . Once the latent classes are determined for each subject  $i$ , the time-to-event and the longitudinal outcomes are conditionally independent given the latent classes, and therefore generated separately. In particular, the survival outcomes (time-to-event) depend on  $X_3, X_4, X_5$ , and the longitudinal outcomes depend on the latent classes. We give more details below.

### B.1 Covariates

At each simulation run, for each subject  $i$  we draw  $X_{i1}, X_{i2}, X_{i3}, X_{i4}, X_{i5}$  uniformly from  $[0, 1]$ ,  $[0, 1]$ ,  $\{0, 1\}$ ,  $[0, 1]$ , and  $\{1, 2, 3, 4, 5\}$  respectively.

### B.2 Latent classes

We determine class membership based on a multinomial logistic model of  $X_1, X_2$ , with increasing level of concentration on one class. Our latent class membership generation model matches the setup of JLCM, and it approaches the setup of JLCT as the concentration level approaches 1.

For subject  $i$ , we compute the value of a “score” function  $f(w_g, X_{i1}, X_{i2})$ , where  $w_g$  denotes the parameters associated with latent class  $g$ , and  $X_{i1}, X_{i2}$  denote the first two covariates of subject  $i$ . The latent class membership for subject  $i$ ,  $g_i$ , is generated according to two key values: the “majority” class  $g_i^0$ , and the “concentration” level  $p_0$ .

Define the “majority” class as the latent class with largest score for sample  $i$ ,

$$g_i^0 = \arg \max_{g \in \{1, 2, 3, 4\}} f(w_g, X_{i1}, X_{i2}).$$

We consider four types of score functions  $f$ , which correspond to four underlying structures of latent classes: tree partition, linear separation, non-linear separation, and asymmetric tree partition. The structure is reflected by the dependency of  $g_i^0$  on  $X_1, X_2$ , which is shown in Figure 1.

The latent class membership of subject  $i$  is drawn according to the probabilities

$$\Pr(g_i = g \mid X_i, C) = \frac{\exp\{Cf(w_g, X_{i1}, X_{i2})\}}{\sum_{l=1}^4 \exp\{Cf(w_l, X_{i1}, X_{i2})\}},$$

where the parameter  $C$  is chosen such that the probability of “major” class is approximately equal to a pre-specified concentration level  $p_0 \in \{0.25, 0.5, 0.7, 0.85, 1\}$ . That is  $\Pr(g_i = g_i^0 \mid X_i, C) \approx p_0$ . In particular, when  $C = 0$ ,  $\Pr(g_i = g_i^0) = 0.25$ , and therefore the latent class membership is randomly determined and independent of  $X_1, X_2$ . On the other hand, when  $C = \infty$ ,  $\Pr(g_i = g_i^0) = 1$ , and therefore the latent class membership corresponds to a deterministic partitioning based on  $X_1, X_2$ , which is consistent with the assumptions underlying a tree partitioning.

The choices of parameters are given below.

- Tree. Consider the following coefficients  $(w_{g1}, w_{g2})$ :

$$\begin{aligned} w_{11} &= -1, & w_{12} &= -1 \\ w_{21} &= -1, & w_{22} &= 1, \\ w_{31} &= 1, & w_{32} &= -1, \\ w_{41} &= 1, & w_{42} &= 1. \end{aligned}$$

Define the score function

$$f_{\text{tree}}(w_g, X_{i1}, X_{i2}) = w_{g1}(2X_{i1} - 1) + w_{g2}(2X_{i2} - 1),$$

and let  $g_i^0 = \arg \max_g f_{\text{tree}}(w_g, X_{i1}, X_{i2})$  denote the latent class with largest score for sample  $i$ . See Figure 1a for the dependency of  $g_i^0$  on  $X_1, X_2$ . The latent classes are drawn according to the probabilities

$$\Pr(g_i = g \mid X_i, C) = \frac{\exp \{C f_{\text{tree}}(w_g, X_{i1}, X_{i2})\}}{\sum_{l=1}^4 \exp \{C f_{\text{tree}}(w_l, X_{i1}, X_{i2})\}},$$

where the parameter  $C$  is chosen such that  $\Pr(g_i = g_i^0 \mid X_i, C) \approx p_0$ , and  $p_0$  is some pre-specified level  $p_0 \in \{0.25, 0.5, 0.7, 0.85, 1\}$ . In particular, when  $C = 0$ ,  $\Pr(g_i = g_i^0) = 0.25$ ; when  $C = \infty$ ,  $\Pr(g_i = g_i^0) = 1$ .

- Linear. Consider the following coefficients  $(w_{g1}, w_{g2})$  drawn randomly from the unit sphere,

$$\begin{aligned} w_{11} &= 0.8, & w_{12} &= -0.6 \\ w_{21} &= 0.9, & w_{22} &= 0.5, \\ w_{31} &= -0.8, & w_{32} &= 0.6, \\ w_{41} &= 0.5, & w_{42} &= 0.9. \end{aligned}$$

Define the score function

$$f_{\text{linear}}(w_g, X_{i1}, X_{i2}) = w_{g1}(2X_{i1} - 1) + w_{g2}(2X_{i2} - 1),$$

and let  $g_i^0 = \arg \max_g f_{\text{linear}}(w_g, X_{i1}, X_{i2})$ . See Figure 1b for the dependency of  $g_i^0$  on  $X_1, X_2$ . The latent classes are drawn according to the following probabilities

$$\Pr(g_i = g \mid X_i, C) = \frac{\exp \{C f_{\text{linear}}(w_g, X_{i1}, X_{i2})\}}{\sum_{l=1}^4 \exp \{C f_{\text{linear}}(w_l, X_{i1}, X_{i2})\}},$$

with  $C$  again chosen to control the value of  $\Pr(g_i = g_i^0 \mid X_i, C) \approx p_0 \in \{0.25, 0.5, 0.7, 0.85, 1\}$ .

- Nonlinear. We can skip the step of defining the score function  $f$  and the  $C$  value, but directly work with  $g_0$  and  $p_0$ . For each observation, its “most likely” latent class  $g_i^0$  is determined by whether  $(X_{i1}, X_{i2})$  belongs to the circles centered at  $(0, 0)$  and  $(0, 1)$  with radius 0.75 :

$$g_i^0 = \begin{cases} 1, & \{X_{i1}^2 + X_{i2}^2 \leq 0.75^2\} \ \& \ \{X_{i1}^2 + (1 - X_{i2})^2 > 0.75^2\} \\ 2, & \{X_{i1}^2 + (1 - X_{i2})^2 \leq 0.75^2\} \ \& \ \{X_{i1}^2 + X_{i2}^2 > 0.75^2\} \\ 3, & \{X_{i1}^2 + X_{i2}^2 > 0.75^2\} \ \& \ \{X_{i1}^2 + (1 - X_{i2})^2 > 0.75^2\} \\ 4, & \{X_{i1}^2 + X_{i2}^2 \leq 0.75^2\} \ \& \ \{X_{i1}^2 + (1 - X_{i2})^2 \leq 0.75^2\} \end{cases}$$

See Figure 1c for visualization of  $g_i^0$ . The latent classes are drawn according to the following probabilities:

$$\Pr(g_i = g \mid X_i) = p_0 \{g = g_i^0\} + \frac{1 - p_0}{3} \{g \neq g_i^0\},$$

where  $p_0 \in \{0.25, 0.5, 0.7, 0.85, 1\}$ .

- Asymmetric. We can skip the step of defining the score function  $f$  and the  $C$  value, but directly work with  $g_0$  and  $p_0$ . For each observation, its “most likely” latent class  $g_i^0$  is determined by the following asymmetric tree:

$$g_i^0 = \begin{cases} 1, & \{X_{i1} > 0.75\}, \\ 2, & \{X_{i1} \leq 0.75\} \ \& \ \{X_{i2} \leq 0.33\}, \\ 3, & \{X_{i1} \leq 0.75\} \ \& \ \{0.33 < X_{i2} \leq 0.67\}, \\ 4, & \{X_{i1} \leq 0.75\} \ \& \ \{X_{i2} > 0.67\}. \end{cases}$$

See Figure 1d. The latent classes are drawn according to the following probabilities:

$$\Pr(g_i = g \mid X_i) = p_0 \{g = g_i^0\} + \frac{1 - p_0}{3} \{g \neq g_i^0\},$$

where  $p_0 \in \{0.25, 0.5, 0.7, 0.85, 1\}$ .

### B.3 Time-to-event

The survival time (time-to-event)  $T_i$  of subject  $i$  follows the proportional hazards model

$$h(t, \mathbf{X}_i) = h_0(t)e^{b_{g_i 3}X_{i3} + b_{g_i 4}X_{i4} + b_{g_i 5}X_{i5}},$$

where the slope coefficients  $b_{g_i 3}, b_{g_i 4}, b_{g_i 5}$  depend on latent class  $g_i \in \{1, 2, 3, 4\}$  for subject  $i$ .

We use three different distributions for baseline hazards  $h_0(t)$ : exponential, Weibull with decreasing hazards with time (Weibull-D), and Weibull with increasing hazards with time (Weibull-I). We select parameters and slopes such that the mean values of survival time  $T$  across latent classes remain similar across different distributions. The distributions and corresponding parameters for generating time-to-event data are listed below.

- Exponential with  $\lambda = 0.1$ , and slopes are

$$\begin{aligned} b_{13} &= 0, & b_{14} &= 0, & b_{15} &= 0 \\ b_{23} &= 0.56, & b_{24} &= 0.56, & b_{25} &= 0.09, \\ b_{33} &= 0.92, & b_{34} &= 0.92, & b_{35} &= 0.15, \\ b_{43} &= 1.46, & b_{44} &= 1.46, & b_{45} &= 0.24. \end{aligned}$$

- Weibull distribution with shape parameter  $\alpha = 0.9$ , which corresponds to decreasing hazards with time (Weibull-D). The scale parameter is  $\beta = 1$ , and slopes are

$$\begin{aligned} b_{13} &= -1.17, & b_{14} &= -1.17, & b_{15} &= -0.19 \\ b_{23} &= -0.66, & b_{24} &= -0.66, & b_{25} &= -0.11, \\ b_{33} &= -0.55, & b_{34} &= -0.55, & b_{35} &= -0.09, \\ b_{43} &= 0, & b_{44} &= 0, & b_{45} &= 0. \end{aligned}$$

- Weibull distribution with shape parameter  $\alpha = 3$ , which corresponds to increasing hazards with time (Weibull-I). The scale parameter is  $\beta = 2$ , and slopes are

$$\begin{aligned} b_{13} &= -3.22, & b_{14} &= -3.22, & b_{15} &= -0.54 \\ b_{23} &= -2.26, & b_{24} &= -2.26, & b_{25} &= -0.38, \\ b_{33} &= -1.53, & b_{34} &= -1.53, & b_{35} &= -0.26, \\ b_{43} &= 0, & b_{44} &= 0, & b_{45} &= 0. \end{aligned}$$

Left truncation times are generated independently from uniform  $U[0, 1]$ . Right censoring times are generated independently from an exponential distribution, with parameters chosen to reflect light censoring (approximately 20% observations are censored), and heavy censoring (approximately 50% observations are censored).

### B.4 Longitudinal outcomes

The longitudinal outcome  $y$  comes from the following linear mixed-effects model: for subject  $i$  at time  $t$ , let  $g_i$  denote the latent class membership, and

$$y_{it} = u_{g_i} + v_i + \varepsilon_{it}, \quad v_i \sim \mathcal{N}(0, \sigma_v^2), \quad \varepsilon_{it} \sim \mathcal{N}(0, \sigma_e^2),$$

where  $\sigma_v = 0.2, \sigma_e = 0.1$ , and  $u_1 = 0, u_2 = 1, u_3 = 1, u_4 = 2$  are class-specific random intercepts. We assume each subject  $i$  is measured at its entry (left truncation) time, together with multiple intermediate measurement times  $t_{i1}, t_{i2}$ , etc. The number of intermediate measurements for subject  $i$  is generated independently from  $1 + \text{Poisson}(1)$ , thus each subject has at least 2 measurements, and has 3 measurements on average. The intermediate measurement time  $t_{ij}$  is then sampled independently and uniformly between subject  $i$ 's left-truncated and right-censored time,  $t_{ij} \sim U[L_i, T_i]$ . Finally, the data are converted to the LTRC format.

Observe that covariates  $X_1$  and  $X_2$  determine the latent classes, and thus affect the time-to-event and longitudinal outcomes  $y$ . Therefore, time-to-event is correlated with  $y$  if  $X_1$  and  $X_2$  are unknown. On the other hand, conditioning on one of the four latent classes  $g = 1, 2, 3, 4$ , time-to-event and longitudinal outcomes are independent: the former follows a class-specific proportional hazards model and only depends on  $X_3, X_4, X_5$ , while the latter is a constant plus random noise. Therefore, the simulated data satisfy the conditional independence assumption made by both JLCM and JLCT.

## B.5 Methods and predictions

Given the simulated data, JLCT and JLCM use almost the same subsets of covariates in their modeling components:  $\mathbf{X}^s = \{X_3, X_4, X_5\}$  to model time-to-event, and  $\mathbf{X}^f = \mathbf{X}^r = \{X_1, \dots, X_5\}$  for fixed and random effects to model longitudinal outcomes. JLCT uses  $\mathbf{X}^g(\text{JLCT}) = \{X_1, \dots, X_5\}$  to model latent class membership. Since tree-based approaches automatically use interactions between covariates to partition the population, for fair comparison we allow JLCM to include an additional interaction term in modeling latent classes:  $\mathbf{X}^g(\text{JLCM}) = \{X_1, \dots, X_5, X_1X_2\}$ . We use the `Jointlcm` function from the R package `lcm` [Proust-Lima et al., 2017, 2018] to fit JLCM.

We compare four methods on the simulated dataset.

1. A baseline model that treats the entire dataset as one latent class. This is equivalent to JLCT with stopping threshold  $s = \infty$ . After the tree is constructed, we fit a Cox PH model.
2. A JLCT with the stopping threshold  $s = 3.84$ . The tree is pruned to have no more than six terminal nodes, which coincides with the maximal number of latent classes we allow for JLCM. After the tree is constructed, we fit a Cox proportional hazards (PH) model with the same baseline hazard function but different Cox PH slopes across terminal nodes.
3. A JLCT that is the same as the second JLCT, except that both baseline hazard functions and Cox PH slopes differ across terminal nodes.
4. A JLCM, with class-specific slopes and class-specific baseline hazard functions in the survival model. The optimal number of latent classes is chosen from  $\{2, 3, 4, 5, 6\}$  using BIC.

The prediction procedure for JLCT, and therefore for the first three methods, is as follows. Once JLCT returns a tree, each subject  $i$  is assigned to a tree leaf node  $d_i$ . We fit the proportional hazards model (2) to the time-to-event data  $(T_i, \delta_i)$ , with time-invariant covariates  $\mathbf{X}_i^s = \{X_{i3}, X_{i4}, X_{i5}\}$  and slopes  $\eta_{d_i} = (b_{d_i3}, b_{d_i4}, b_{d_i5})$  for  $d_i \in \{1, 2, 3, 4, 5, 6\}$  (since there are no more than six terminal nodes). Method 2 assumes a shared baseline hazard function  $h_0(t)$ , meanwhile Method 3 assumes class-specific baseline hazard functions  $h_{d_i0}(t)$ . We use the R function `coxph` from the `survival` package [Therneau, 2015, Therneau and Grambsch, 2000] to get fitted slopes  $\hat{b}_{d3}, \hat{b}_{d4}, \hat{b}_{d5}$  for all  $d \in \{1, 2, 3, 4, 5, 6\}$ . Given the fitted model, we compute the predicted survival probability for subject  $i$  at time  $t$ , denoted  $\hat{S}_i(t)$ , using the R function `survfit.coxph`. For longitudinal outcomes, we fit the linear mixed-effects model (1) using the R function `lmer` from the `lme4` package [Bates et al., 2015], and compute the predicted longitudinal outcomes  $\hat{y}_{it}$ . For any out-of-sample subject  $k$ , we first determine its leaf node assignment  $d_k$  according to its covariates  $\mathbf{X}_k^s$  and the constructed tree of JLCT. Then we proceed to compute predictions  $\hat{S}_k(t)$  and  $\hat{y}_{kt}$  as we did for the in-sample subjects.

The prediction procedure for JLCM is very similar to that of JLCT. Let  $D^*$  be the BIC optimal number of latent classes. For each latent class  $d \in \{1, \dots, D^*\}$ , JLCM returns estimated Cox PH coefficients  $\hat{b}_{d3}, \hat{b}_{d4}, \hat{b}_{d5}$  as well as the baseline survival curves  $\hat{S}_{d0}(t)$ . In addition, JLCM returns a fitted linear mixed-effects model for longitudinal outcomes. For in-sample subjects, JLCM also returns a predicted latent class membership  $d_i$  for each subject  $i$ , conditioning on all available information: covariates  $\mathbf{X}_i$ , time-to-event  $(T_i, \delta_i)$ , and longitudinal outcomes  $\mathbf{Y}_i$ . We can therefore use the estimated parameters for class  $d_i$  to compute  $\hat{S}_i(t)|_{d_i}$  and  $\hat{y}_{it}|_{d_i}$ . Note that JLCM uses much more information than JLCT at the prediction time to determine the latent class memberships for in-sample subjects, and thus JLCM is expected to perform better than JLCT on in-sample data. For any new subject  $k$ , however, time-to-event and longitudinal outcomes are no longer available at prediction time. Instead, we use JLCM's fitted multinomial logistic model to get  $\pi_k = (p_{k1}, \dots, p_{kD^*})$ , a vector of predicted probabilities of subject  $k$  belonging to each latent class. Finally we take weighted averages over all classes as final predictions:

$$\hat{S}_k(t) = \sum_{d=1}^{D^*} p_{kd} \hat{S}_k(t)|_d, \quad \hat{y}_k(t) = \sum_{d=1}^{D^*} p_{kd} \hat{y}_{kt}|_d.$$

## C Simulation setup: time-varying covariates

In this section we give details of the data generating scheme in the simulation study of time-varying covariates (Section 4).

## C.1 Covariates

At each simulation run, for each subject  $i$  we randomly generate five independent, time-varying covariates  $X_{it1}, \dots, X_{it5}$ , which are piecewise constant, and change values at time  $t_i$ . To be more concrete, for each subject  $i$ , we first randomly generate a time point  $t_i \sim U[1, 3]$ . Next, draw  $X'_{i1}, X'_{i2}, X'_{i3}, X'_{i4}, X'_{i5}$  uniformly from  $[0, 1]$ ,  $[0, 1]$ ,  $\{0, 1\}$ ,  $[0, 1]$ , and  $\{1, 2, 3, 4, 5\}$  respectively. Generate  $X''_{i1}, X''_{i2}, X''_{i3}, X''_{i4}, X''_{i5}$  by

$$\begin{aligned} X''_{i1} &= \text{Proj}_{[0,1]}(X'_{i1} + U[-0.3, 0.3]), \\ X''_{i2} &= \text{Proj}_{[0,1]}(X'_{i2} + U[-0.3, 0.3]), \\ X''_{i3} &= U\{0, 1\}, \\ X''_{i4} &= \text{Proj}_{[0,1]}(X'_{i4} + U[-0.3, 0.3]), \\ X''_{i5} &= \text{Proj}_{[1,5]}(X'_{i5} + U\{-1, 0, 1\}), \end{aligned}$$

where the projection operator  $\text{Proj}_{[a,b]}(x)$  projects any real value  $x$  onto the interval  $[a, b]$ . For example,  $\text{Proj}_{[0,1]}(1.3) = 1$ . For  $k \in \{1, 2, 3, 4, 5\}$ , the time-varying covariate  $X_k$  of object  $i$  at time  $t$  is defined as

$$X_{itk} = 1\{t \leq t_i\}X'_{ik} + 1\{t > t_i\}X''_{ik}.$$

Therefore, for each subject  $i$ , the five time-varying covariates  $X_1, \dots, X_5$  are piecewise constant, and change values at time point  $t_i$ .

## C.2 Latent classes

We use the same procedure as is described in Appendix B to generate latent classes, the only difference being that the covariates  $X_1, X_2$  become time-varying, as does the latent class membership. We denote by  $g_{it}$  the latent class membership of subject  $i$  at time  $t$ .

## C.3 Time-to-event

The time-to-event data follow the same hazard models as in Appendix B, except that the covariates and slope coefficients are time-varying. The hazard of subject  $i$  at time  $t$  becomes

$$h(t, \mathbf{X}_i) = h_0(t)e^{b_{g_{it}3}X_{it3} + b_{g_{it}4}X_{it4} + b_{g_{it}5}X_{it5}},$$

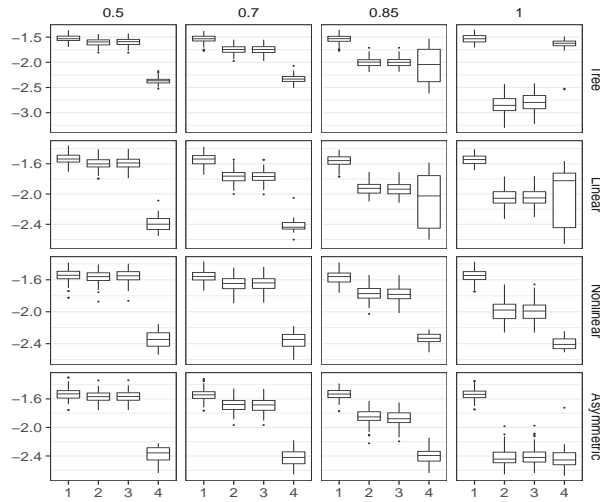
where the slope coefficients  $b_{g_{it}3}, b_{g_{it}4}, b_{g_{it}5}$  depend on latent class membership  $g_{it} \in \{1, 2, 3, 4\}$  at time  $t$ .

## C.4 Longitudinal outcomes

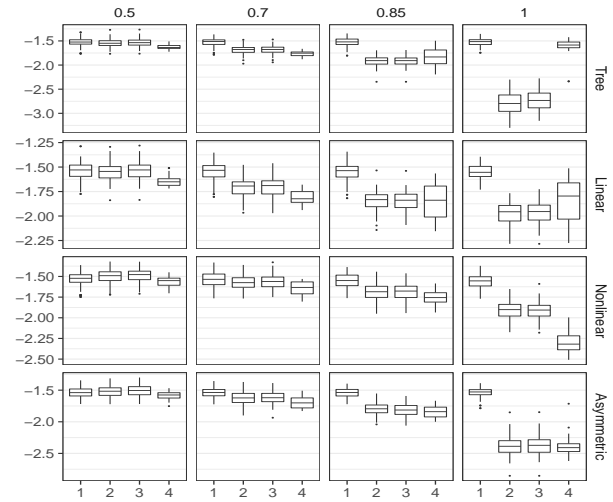
The longitudinal outcome  $y$  follows the same linear mixed-effects model as in Appendix B, the only difference being now the fixed effect  $u_{g_{it}}$ , which depends on the latent class membership  $g_{it}$ , becomes time-varying as well.

## D Additional simulation results: time-invariant covariates

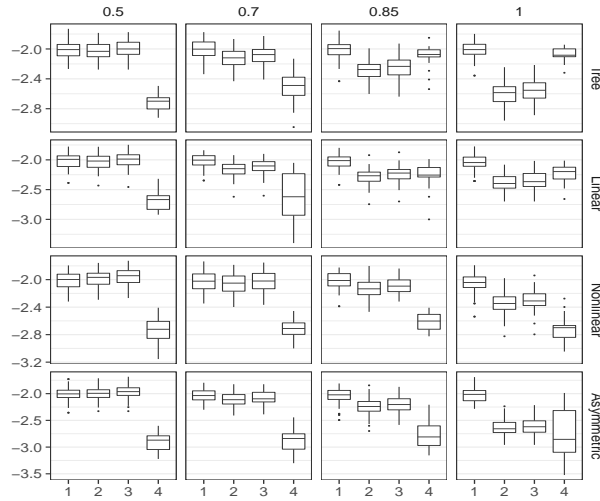
In this section, we present the complete simulation results: for three time-to-event distributions (Weibull-I, Weibull-D, and Exponential), and light censoring. The results of other censoring levels (no censoring, heavy censoring) are very similar to those of light censoring, and are omitted. We report results for the four methods discussed in Section 3: (1) JLCT with no split, (2) JLCT with same baseline hazard function but different Cox PH slopes across terminal nodes, (3) JLCT with different baseline hazard function and different Cox PH slopes across terminal nodes, and (4) JLCM with different baseline hazard function and different Cox PH slopes across terminal nodes, using an interaction term in modeling latent class membership. We use the performance measures described in Section 3:  $\text{ISE}_{\text{in}}$ ,  $\text{ISE}_{\text{out}}$ ,  $\text{MSE}_{y_{\text{in}}}$ ,  $\text{MSE}_{y_{\text{out}}}$ , and  $\text{MSE}_b$ .



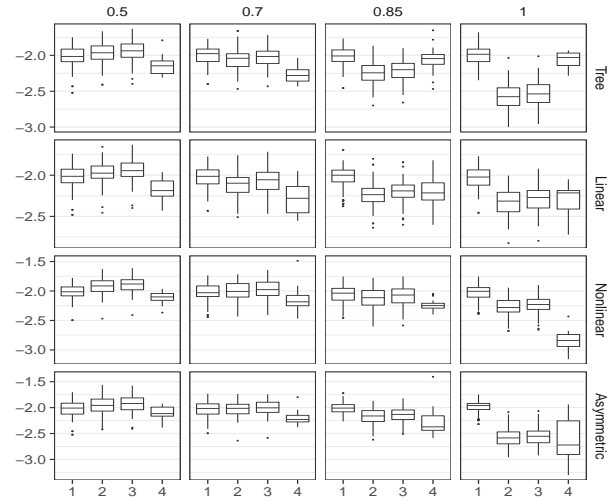
(a) Weibull-I,  $ISE_{in}$



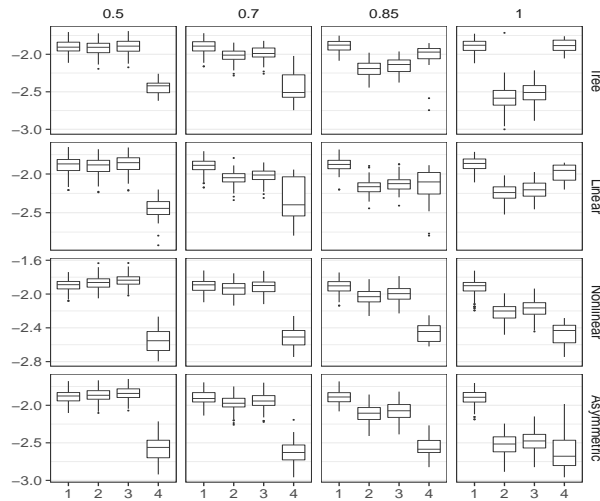
(b) Weibull-I,  $ISE_{out}$



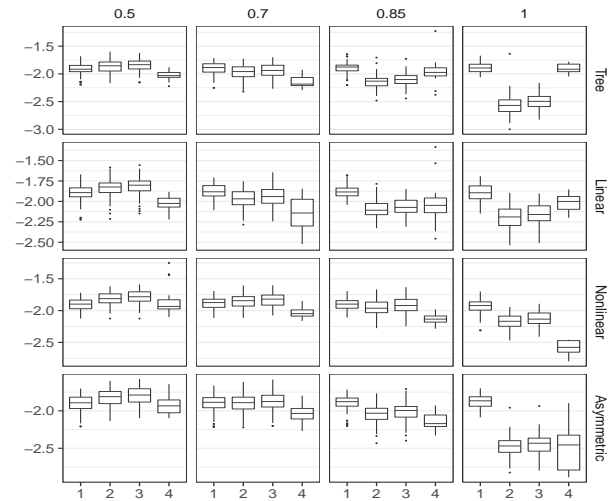
(c) Weibull-D,  $ISE_{in}$



(d) Weibull-D,  $ISE_{out}$



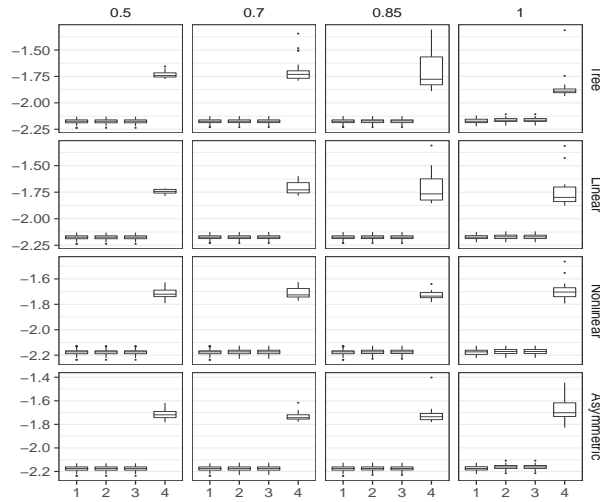
(e) Exponential,  $ISE_{in}$



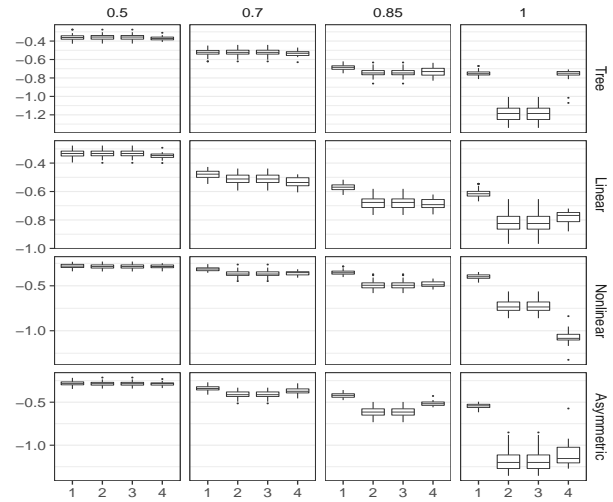
(f) Exponential,  $ISE_{out}$

Figure 5: Boxplots of integrated squared error (ISE, both in-sample and out-of-sample) on  $\log_{10}$  scale, time-invariant covariates,  $N=500$ , light censoring, Weibull-I, Weibull-D, and Exponential distribution.

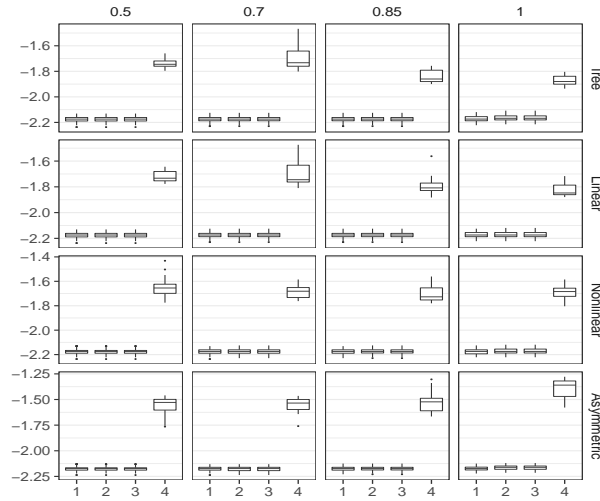




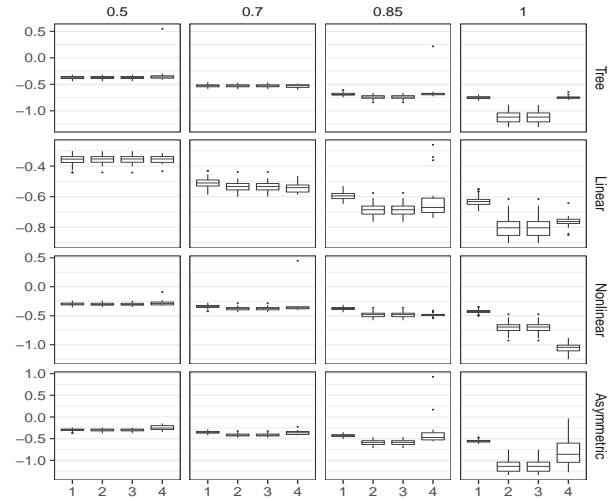
(a) Weibull-I,  $MSE_{y_{in}}$



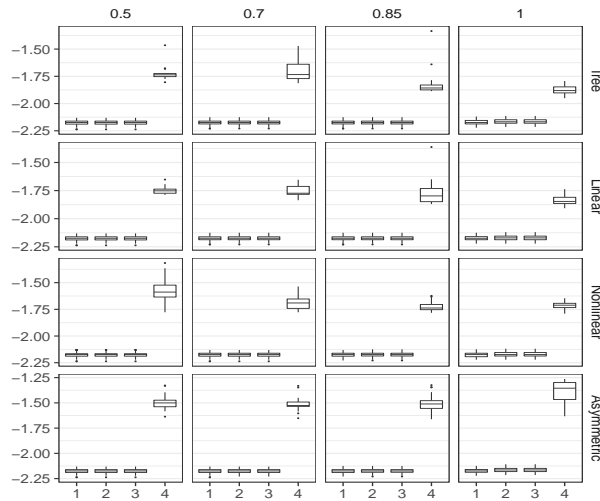
(b) Weibull-I,  $MSE_{y_{out}}$



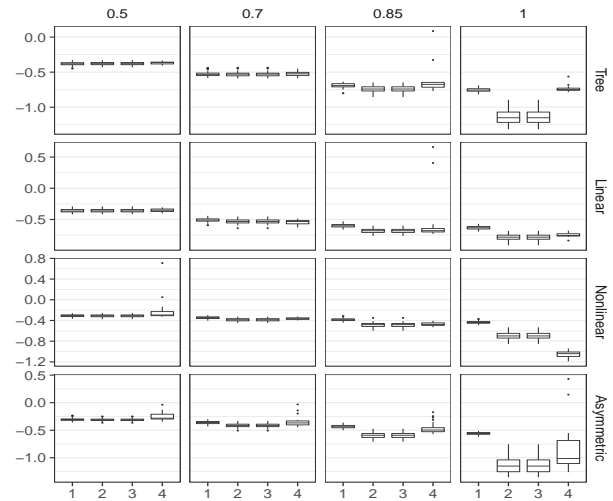
(c) Weibull-D,  $MSE_{y_{in}}$



(d) Weibull-D,  $MSE_{y_{out}}$

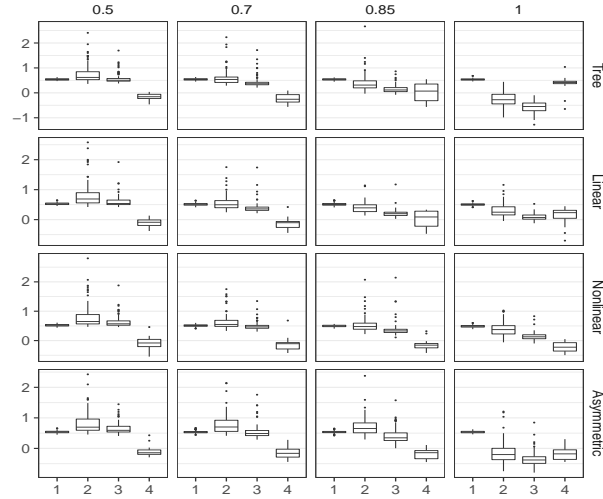


(e) Exponential,  $MSE_{y_{in}}$

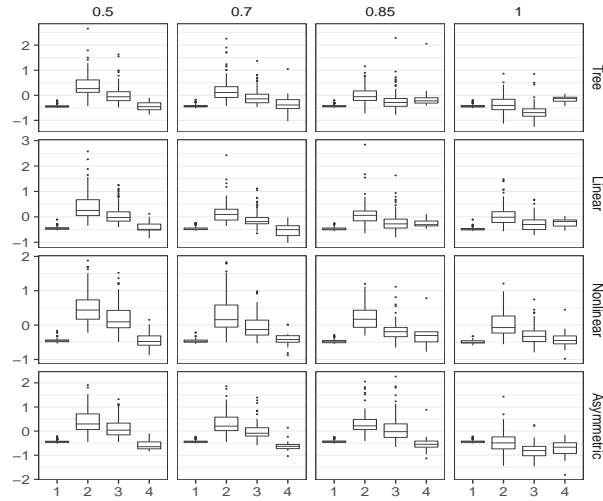


(f) Exponential,  $MSE_{y_{out}}$

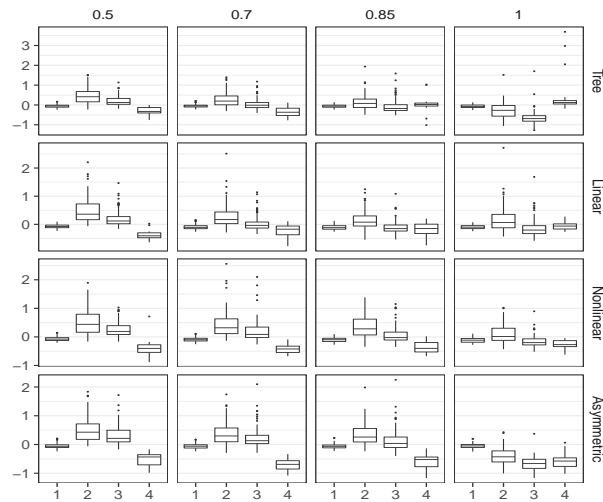
Figure 6: Boxplots of mean squared error ( $MSE_y$ , both in-sample and out-of-sample) on  $\log_{10}$  scale, time-invariant covariates,  $N=500$ , light censoring, Weibull-I, Weibull-D, and Exponential distribution.



(a) Weibull-I,  $MSE_b$



(b) Weibull-D,  $MSE_b$

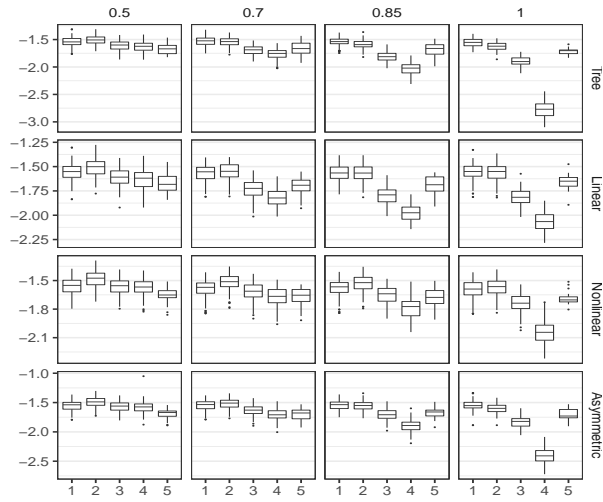


(c) Exponential,  $MSE_b$

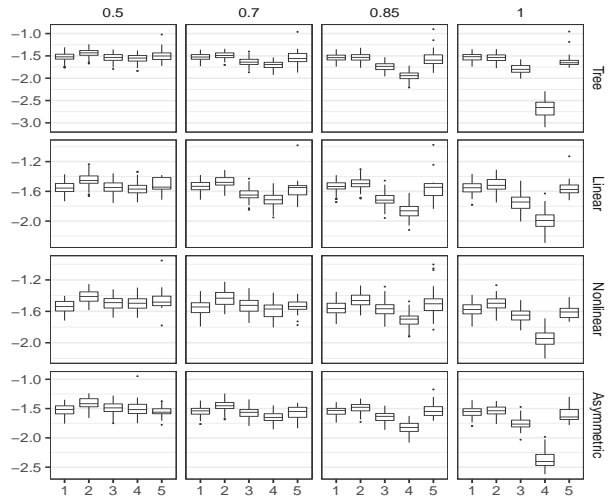
Figure 7: Boxplots of mean squared error ( $MSE_b$ ) of estimated Cox PH slopes, on  $\log_{10}$  scale, time-invariant covariates,  $N=500$ , light censoring, Weibull-I, Weibull-D, and Exponential distribution.

## E Additional simulation results: time-varying covariates

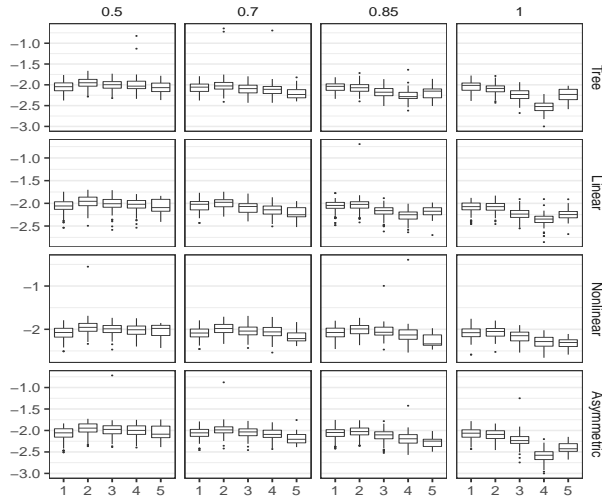
In this section, we present the complete simulation results for time-varying covariates: for three time-to-event distributions (Weibull-I, Weibull-D, and Exponential), and light censoring. No censoring and heavy censoring are omitted because of their similar performances to light censoring. We report results for the five methods discussed in Section 4: (1) JLCT with no split, and using time-varying survival covariates, (2) JLCT with “time-invariant” latent class and survival covariates, (3) JLCT with “time-invariant” latent class covariates and time-varying survival covariates, (4) JLCT with time-varying latent class and survival covariates, and (5) JLCM with “time-invariant” latent class and survival covariates. We use the performance measures described in Section 3:  $ISE_{in}$ ,  $ISE_{out}$ ,  $MSE_{y_{in}}$ ,  $MSE_{y_{out}}$ , and  $MSE_b$ .



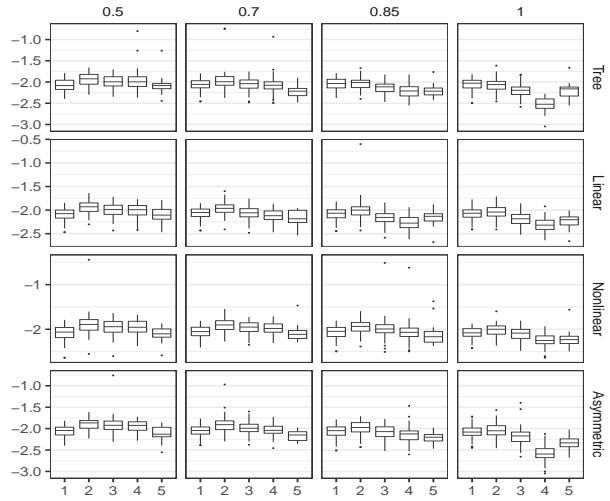
(a) Weibull-I,  $ISE_{in}$



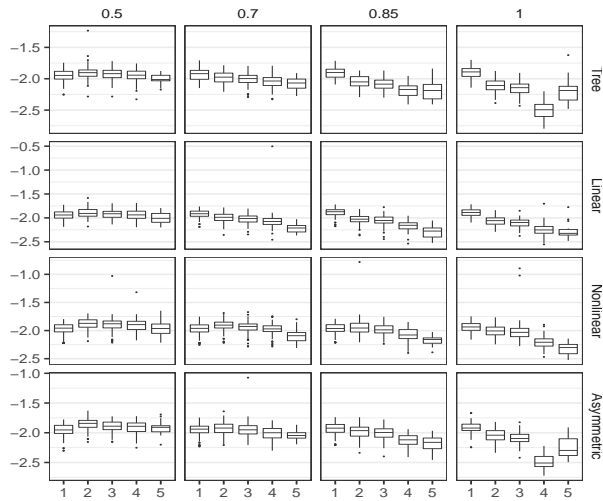
(b) Weibull-I,  $ISE_{out}$



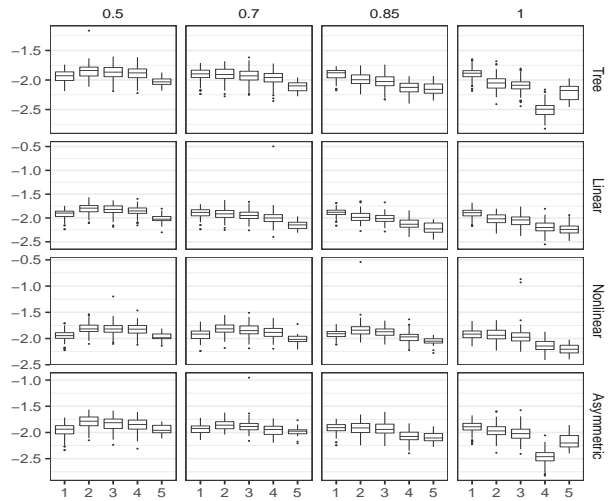
(c) Weibull-D,  $ISE_{in}$



(d) Weibull-D,  $ISE_{out}$

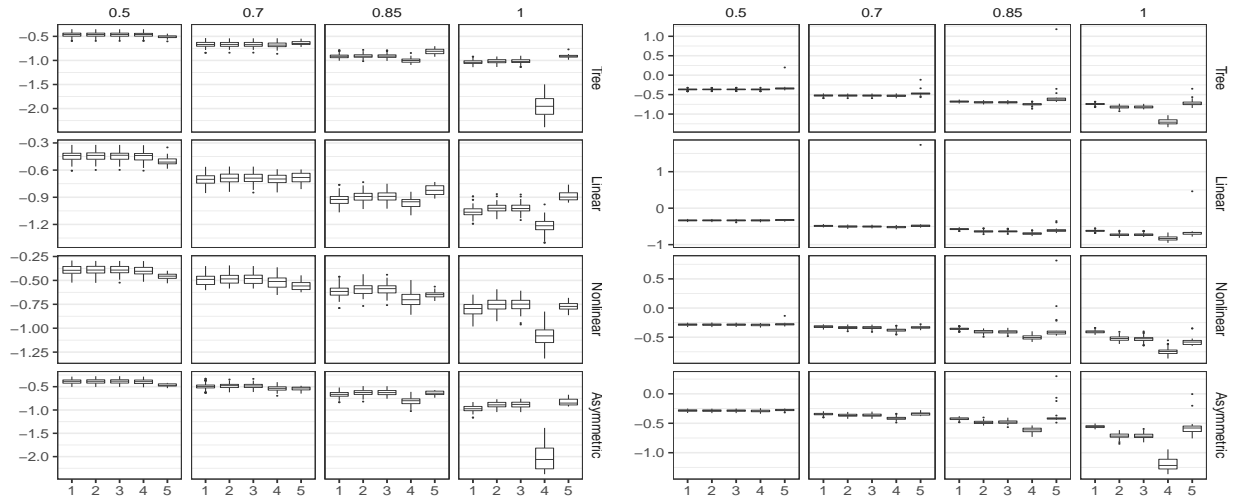


(e) Exponential,  $ISE_{in}$



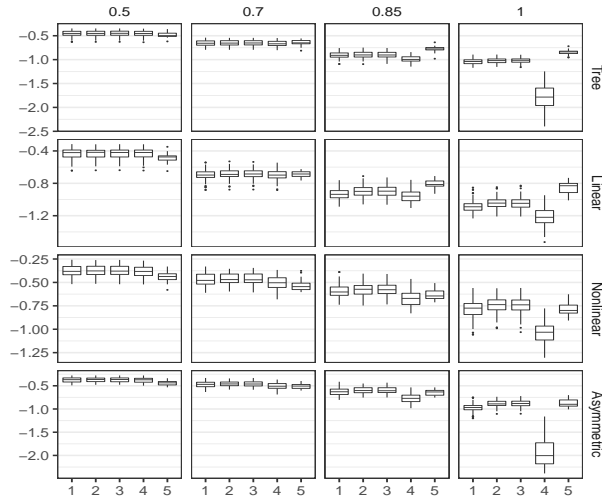
(f) Exponential,  $ISE_{out}$

Figure 8: Boxplots of integrated squared error (ISE, both in-sample and out-of-sample) on  $\log_{10}$  scale, time-varying covariates,  $N=500$ , light censoring, Weibull-I, Weibull-D, and Exponential distribution.

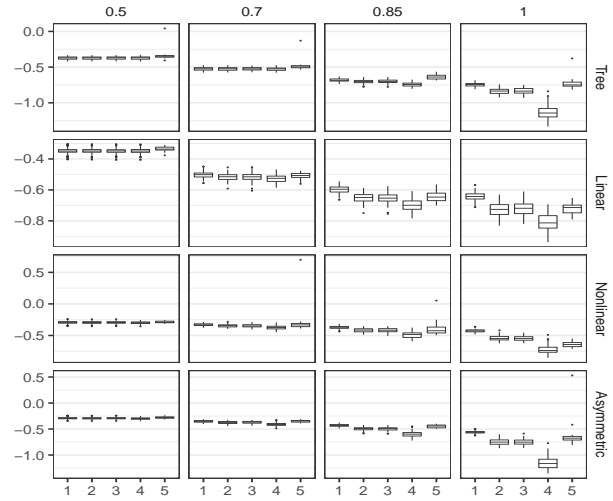


(a) Weibull-I,  $MSE_{y_{in}}$

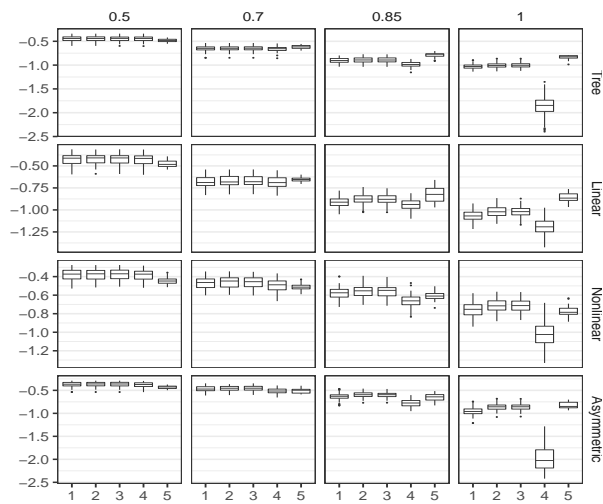
(b) Weibull-I,  $MSE_{y_{out}}$



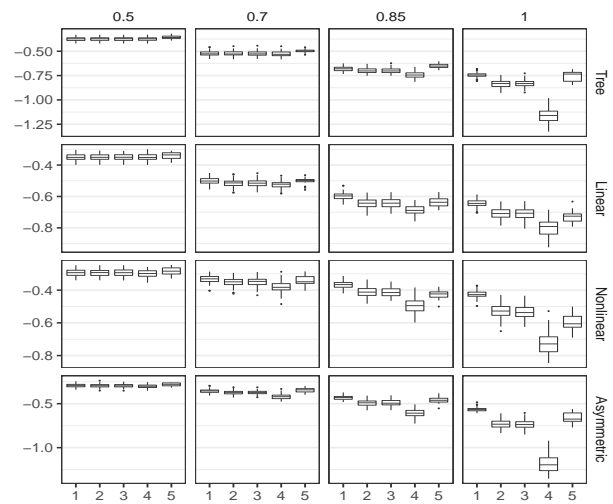
(c) Weibull-D,  $MSE_{y_{in}}$



(d) Weibull-D,  $MSE_{y_{out}}$

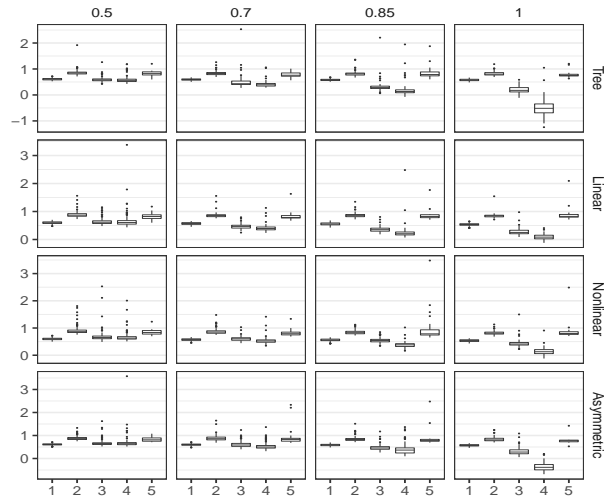


(e) Exponential,  $MSE_{y_{in}}$

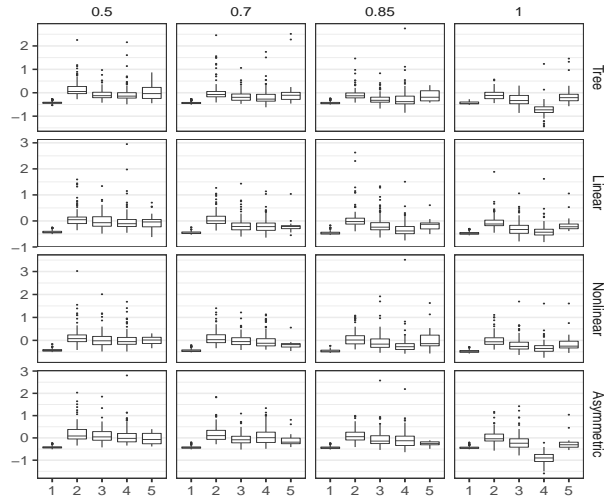


(f) Exponential,  $MSE_{y_{out}}$

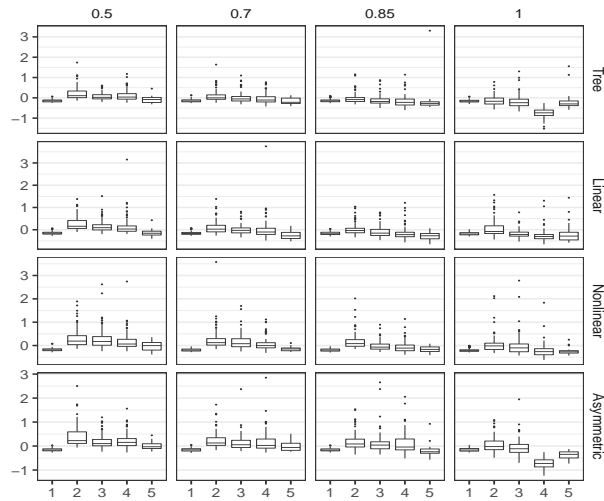
Figure 9: Boxplots of mean squared error ( $MSE_y$ , both in-sample and out-of-sample) on  $\log_{10}$  scale, time-varying covariates,  $N=500$ , light censoring, Weibull-I, Weibull-D, and Exponential distribution.



(a) Weibull-I,  $MSE_b$



(b) Weibull-D,  $MSE_b$



(c) Exponential,  $MSE_b$

Figure 10: Boxplots of mean squared error ( $MSE_b$ ) of estimated Cox PH slopes, on  $\log_{10}$  scale, time-varying covariates,  $N=500$ , light censoring, Weibull-I, Weibull-D, and Exponential distribution.

## F Using the R package `jlctree`

In this section, we demonstrate how to use the R package `jlctree` to fit JLCT to a simulated dataset and to the PAQUID dataset. For more details about the `jlctree` package, please refer to the package manual available at CRAN.

The `jlctree` package includes an example dataset, `data_timevar`, which is generated under the time-varying setup described in Section 4. The call of `jlctree` to fit JLCT (Method 4 in Section 4) to `data_timevar` is

---

```
library(jlctree)
data(data_timevar)
tree <- jlctree(survival=Surv(time_L, time_Y, delta)~X3+X4+X5,
               classmb=~X1+X2, fixed=y~X1+X2+X3+X4+X5, random=~1,
               subject='ID', data=data_timevar,
               parms=list(maxng=4))
```

---

Next, we reproduce the results of JLCT on the PAQUID dataset. We first convert the original PAQUID dataset (contained in the R package `lcmm`) into left-truncated right-censored (LTRC) format.

---

```
library(lcmm)
library(NormPsy)
library(data.table)
paquid$normMMSE <- normMMSE(paquid$MMSE)
paquid$age65 <- (paquid$age - 65) / 10
paquidS <- paquid[paquid$agedem > paquid$age_init & paquid$age <= paquid$agedem, ]
paquidS2 <- data.table(paquidS)
paquidS2$age <- paquidS2[, {if(.N==1){age_init}
                          else {c(age_init[1], age[c(1:(.N-1)])}}}, by=ID] [, V1]
temp <- subset(paquidS2, select=c(ID, age_init, agedem, dem, male))
temp <- unique(temp)
data <- tmerge(temp, temp, id=ID, tstart=age_init,
              tstop=agedem, death = event(agedem, dem))
data <- tmerge(data, paquidS2, id=ID, age65 = tdc(age, age65),
              CEP= tdc(age, CEP), normMMSE=tdc(age, normMMSE),
              BVRT=tdc(age, BVRT), IST=tdc(age, IST),
              HIER=tdc(age, HIER), CESD=tdc(age, CESD))
data <- subset(data, !is.na(normMMSE) & !is.na(BVRT)
              & !is.na(IST) & !is.na(HIER) & !is.na(CESD))
```

---

The R code that fits JLCT to the PAQUID dataset using the time-varying covariates, and plots the obtained tree structure as in Figure 4c, is

---

```
library(jlctree)
library(rpart.plot)
data$age <- round(10*data$age65+65)
tree_var <- jlctree(survival=Surv(tstart, tstop, death)~CEP+male+
                  BVRT+IST+HIER+CESD+poly(age_init, degree=2, raw=TRUE),
                  classmb=~CEP+male+age+BVRT+IST+HIER+CESD,
                  fixed=normMMSE~CEP+poly(age65, degree=2, raw=TRUE),
                  random=~poly(age65, degree=2, raw=TRUE),
                  subject='id', data=data,
                  parms=list(min_nevent=5, fits=F, fity=F))
rpart.plot(tree_var$tree)
```

---

One can fit JLCT to the PAQUID dataset using the time-invariant covariates by changing the corresponding arguments in the above `jlctree` call.